ADDITIONAL DETERMINISTIC EVALUATIONS PERFORMED TO ASSESS SEISMIC MARGINS OF THE DIABLO CANYON POWER PLANT UNITS 1 AND 2

September 1990

This volume responds to deterministic evaluation questions asked of PG&E by the U. S. Nuclear Regulatory Commission (NRC) staff in their letter of April 26, 1990, and during discussions at the NRC/PG&E May 8, 1990 meeting. These responses provide data requested to augment information presented in the Final Report of the Long Term Seismic Program, submitted by PG&E to the NRC on July 31, 1988.

PREFACE

PG&E's response to the NRC Staff's April 1990 request for additional information regarding the Diablo Canyon Long Term Seismic Program deterministic evaluations is contained in this volume. The reply to the request is included in the responses to nine questions we have formulated to best describe the additional deterministic evaluations performed to augment the information contained in Chapters 7 and 8 of the Long Term Seismic Program Final Report. The NRC Staff's general request precedes Question DE 1.

The responses to Questions DE 1 through DE 3 describe the evaluation work scope and the methods we used to define the maximum magnitude earthquake inputs to the Plant power block structures and the procedure for developing global and local seismic responses (demands) on the primary load resisting elements. Questions DE 4 through DE 6 provide comparisons of maximum magnitude earthquake demands with the Hosgri demands and capacities of selected structural elements, a comparison with structural element capacities based on the conservative deterministic failure margin approach, and seismic margins for these structural elements. The attachment to Question DE 6 contains a discussion of the conservative deterministic failure margin approach and its application to the Diablo Canyon evaluations, as well as an explanation of seismic margins. The response to Question DE 7 provides a deterministic evaluation of the fuel handling building crane. A description of the methods used to reassess the seismic capacity of the containment fan cooler and diesel generator control panel is provided in response to Question DE 8. The response to Question DE 9 provides the conclusions we have reached regarding these additional deterministic evaluations and the adequacy of Plant seismic margins. The contents of this volume are organized as follows:

Contents

SUMMARY

This volume describes the additional deterministic evaluations Pacific Gas and Electric Company (PG&E) has performed as part of the Long Term Seismic Program for Diablo Canyon Power Plant Units 1 and 2 in response to an NRC Staff request in April 1990. The studies augment the deterministic evaluations and seismic margin assessments presented in Chapters 7 and 8 of the Final Report (PG&E, 1988) submitted to the Nuclear Regulatory Commission in July 1988 in satisfaction of License Condition 2.C.(7) for Unit 1. The scope of these additional deterministic evaluations was agreed upon in a meeting between the NRC Staff and PG&E on May 8, 1990.

Two major approaches are used to calculate high-confidence-of-low-probability-of-failure (HCLPF) capacity estimates for structures and components: the fragility analysis method and the conservative deterministic failure margin (CDFM) approach. PG&E's seismic probabilistic risk assessment reported in PG&E, 1988 used HCLPF capacity values derived from the fragility analysis method. The purpose of the additional evaluations in this volume was to quantify seismic capacity values for power block structures and selected components using the CDFM approach and to compare the results with spectral acceleration capacity values previously computed using the fragility analysis method. The structures and components were selected for reassessment (called the "screened-in" structures and components, EPRI, 1988) based on the following:

- Seismic probabilistic assessment studies identified the structures or components that are the highest contributors to the seismic risk (e.g., the turbine building and diesel generator control cabinet).

- Major structures particularly important to plant safety are included (e.g., the containment and auxiliary buildings).

- Special and unique structural and seismic response issues that make the specific structures and components good candidates for special evaluation (e.g., the fuel handling building crane and containment fan cooler anchorage).

In order to have a common basis for comparison, we used the same 1988 84th-percentile, site-specific, maximum magnitude earthquake response spectra that were used for the seismic margin assessments described in PG&E, 1988. In addition, consistent with the recommended industry practice (EPRI, 1988), the CDFM approach used a set of conservative, deterministic considerations and factors (e.g., seismic demands, damping, material strength, strength equations, and ductility) to produce conservative results for the seismic capacities (HCLPF) of the structures and components. Also, consistent with the conservative recommendation in the CDFM approach, we have combined the small-break loss-of-coolant-accident pressure with the site-specific ground motions.

In addition to establishing seismic margins by the CDFM approach, and in accordance with the NRC's request, we have reported the building forces such as base shear, overturning moments, and torsion for the containment, auxiliary, and turbine buildings due to the maximum magnitude earthquake and compared these forces with the corresponding forces and capacities based on the Hosgri reevaluation criteria. These comparisons are provided in response to Questions DE 4 and DE 5. As described in the response to Question DE 6, the building capacities were determined to have ample seismic margin.

It should be noted that the objective of the Plant qualification evaluations, including the reevaluation for

the Hosgri earthquake, was to demonstrate that structures meet or exceed specified criteria, and not to quantify seismic margins. The Plant seismic qualification basis methods contain various degrees of conservatism. Different strength evaluation methods were used for the evaluation of different buildings consistent with the licensing criteria. For example, the evaluation of shear walls in the turbine building was performed using Structural Engineers Association of California (1974) strength equations; those of the auxiliary building were performed using a set of project-specific criteria. Thus, comparison of maximum magnitude earthquake demands and Hosgri capacities, while of interest, cannot and should not be used as a basis for determining seismic margins.

The evaluations confirm that the seismic capacities of the critical structures and components estimated by the CDFM approach compare reasonably well with those previously estimated using the fragility analysis method and, therefore, our conclusions regarding seismic risk and the adequacy of seismic margins reported in PG&E, 1988 remain unchanged. Specifically:

- The turbine building was previously identified as the most critical structure with a seismic margin of at least 14 percent, and most likely in excess of 40 percent. The CDFM approach has demonstrated that the seismic margin is indeed in excess of 40 percent.

- The containment building shell was previously estimated to have seismic margin of at least 100 percent. The CDFM approach shows that the seismic margin is approximately 80 percent.

- The auxiliary building was previously estimated to have a seismic margin of at least 70 percent. The conservative deterministic failure margin approach shows that the seismic margin is indeed in excess of 70 percent.

- The CDFM approach confirms that the seismic margins for the critical components continue to be in excess of 40 percent.

The seismic margins reported above are extremely conservative since the margins are based on the 84 percent probability of nonexceedance site-specific spectrum for the maximum magnitude earthquake. The ratio of the 84 to 50 percent spectrum is approximately 1.5. Also, there is margin above the conservative $HCLPF_{84}$ capacity values. The median capacity, which corresponds to the 50 percent probability of exceedance, is generally at least a factor of 2 greater than the $HCLPF_{84}$ capacity. For example, when the $HCLPF_{84}$ spectral acceleration equals the average spectral acceleration for the 84 percent, site-specific spectrum (that is, there is a 0 percent margin), the median capacity will still be approximately a factor of 3 (2 x 1.5) above the 50 percent site-specific spectrum. Thus, a 0 percent deterministic margin obtained in this manner corresponds to a very remote possibility of failure.

REFERENCES

Electric Power Research Institute, 1988, A methodology for assessment of nuclear power plant seismic margin: EPRI NP-6041.

Pacific Gas and Electric Company, 1988, Final report of the Diablo Canyon Long Term Seismic Program: Docket No. 50-275 and 50-323.

There is general agreement on the methodology used in Chapter 7 of the Long Term Seismic Program Final Report to show that the plant structures and components have adequate seismic margins over the demands (plant responses) resulting from the 84th-percentile ground motions due to the maximum magnitude earthquake. However, the scope of the deterministic evaluations reported in the Final Report should be expanded to include the following additional items:

1. *Compare the Hosgri-estimated structural response parameters with similar LTSP response parameters for Category I structures.*

2. *Compare the LTSP deterministic capacities with those predicted by the Hosgri analysis for selected structural elements and components.*

3. *For selected items, provide capacities made using the Conservative Deterministic Failure Margin (CDFM) method.*

QUESTION DE 1

Provide the scope of the additional deterministic evaluations performed to augment the evaluations described in Chapter 7 of the LTSP Final Report.

PG&E met with the NRC Staff on May 8, 1990, in a public meeting to discuss the scope and criteria for the additional deterministic evaluations. Following the meeting, we documented our understanding of the agreement reached regarding the evaluation work scope and procedure (PG&E, 1990). The scope of the additional deterministic evaluations included the following structures and equipment:

- Containment building
  - Global base shear and overturning moment
  - Shell; responses at one or two locations
  - Interior structure; responses at one or two locations
- Auxiliary building[1]
  - Global base shear and overturning moment
  - Shear walls; responses of one or two major walls
- Turbine building[1]
  - Shear walls; responses of one or two major walls
- Fuel handling building crane

[1] The masonry block walls in the auxiliary and turbine buildings, originally included in PG&E, 1990, are being addressed by other reassessment activities requested by the NRC Staff.

- Containment fan cooler (anchorage)
- Diesel generator control panel (critical failure mode)

These structures and equipment were selected for seismic margin reassessment based on the following considerations:

- Major structure important to plant safety.
- Governing capacity based on fragility studies described in the 1988 Final Report.
- Sensitive to seismic vertical loadings.
- Sensitive to anchorage failure mode.
- Equipment fragility based on results of a seismic testing program.

The additional deterministic evaluations described in PG&E, 1990 can be summarized as follows:

- Shear forces and overturning/bending moments for the maximum magnitude earthquake ground motion response spectra would be compared with the corresponding responses determined for the Hosgri reevaluation.
- For those cases where the maximum magnitude earthquake response exceeds the Hosgri response for a particular structural element, the maximum magnitude earthquake response would be compared with the capacity of the structural element established for the Hosgri reevaluation. The responses would be computed for the same load combinations as those used for the Hosgri reevaluation.
- For those structural elements where the maximum magnitude earthquake responses using the Hosgri load combinations exceed the Hosgri capacities, seismic margins would be evaluated using conservative deterministic failure margin (CDFM) criteria and appropriate load combinations.

Although we committed to perform deterministic evaluations for one or two walls in the auxiliary building and the turbine building, it became clear during the evaluation that additional walls were required to be assessed for a better understanding of the performance of these buildings. Thus, the scope of the evaluations was expanded to include additional shear walls in these buildings. The comparisons and margin evaluations identified in the procedure steps above were performed and documented for all cases evaluated; that is, even for those cases where the maximum magnitude earthquake responses did not exceed the Hosgri response or Hosgri capacity.

REFERENCES

Pacific Gas and Electric Company, 1990, letter No. DCL-90-137 to U. S. Nuclear Regulatory Commission: Long Term Seismic Program - Deterministic Evaluations.

QUESTION DE 2

Describe the seismic ground motions that were used for the additional deterministic evaluations of the Plant structures.

The seismic ground motion input data were the 84th-percentile, 5 percent damped, horizontal and vertical site-specific acceleration response spectra defined in the Diablo Canyon Long Term Seismic Program Final Report (PG&E, 1988) for the maximum magnitude earthquake. These spectra are shown in Figures DE Q2-1 and DE Q2-2.

Two sets of two-component actual earthquake horizontal ground motion time-histories of the Pacoima Dam records of the 1971 San Fernando earthquake and the 1978 Tabas earthquake were adjusted to closely match the prescribed site-specific ground motion horizontal response spectrum. The adjustment procedure was the same as described in Chapter 5 of PG&E, 1988. The 5 percent damped response spectra of the time-histories thus modified are compared with the 84th-percentile, site-specific spectrum in Figures DE Q2-3 through DE Q2-6 for the Pacoima Dam and Tabas longitudinal and transverse motions.

The average modified horizontal time-history response spectrum for Pacoima Dam and Tabas (obtained by averaging the four input ground spectra) is compared with the 84th-percentile, site-specific spectrum in Figure DE Q2-7. Exceedances of the average response spectrum over the "target" spectrum were established at frequency ranges of interest and determined to be more than 5 percent.

REFERENCES

Pacific Gas and Electric Company, 1988, Final report of the Diablo Canyon Long Term Seismic Program: U. S. Nuclear Regulatory Commission, Docket Nos. 50-275 and 50-323.

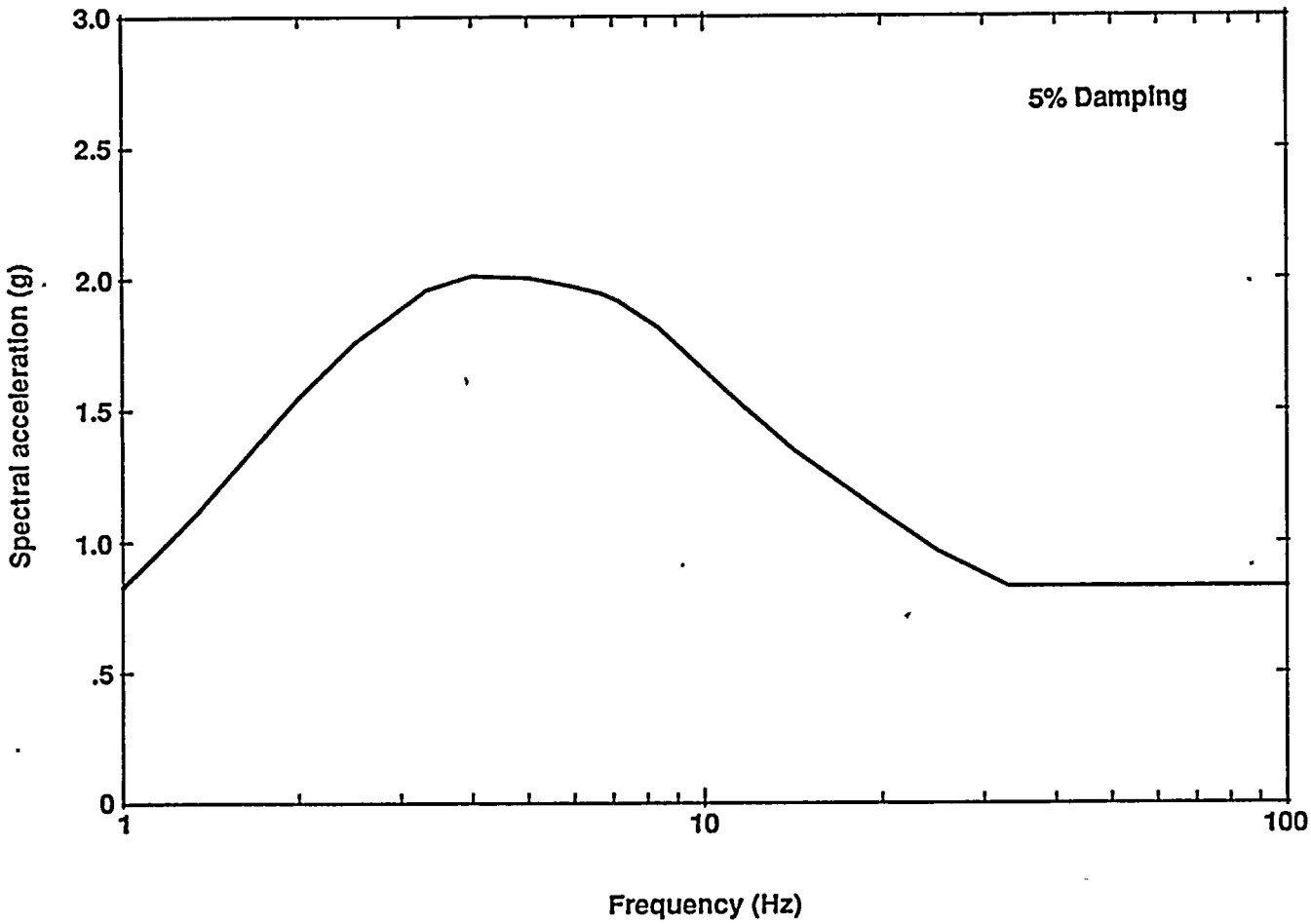

Figure DE Q2-1

84th-percentile, site-specific horizontal ground motion response spectrum for the maximum magnitude earthquake.

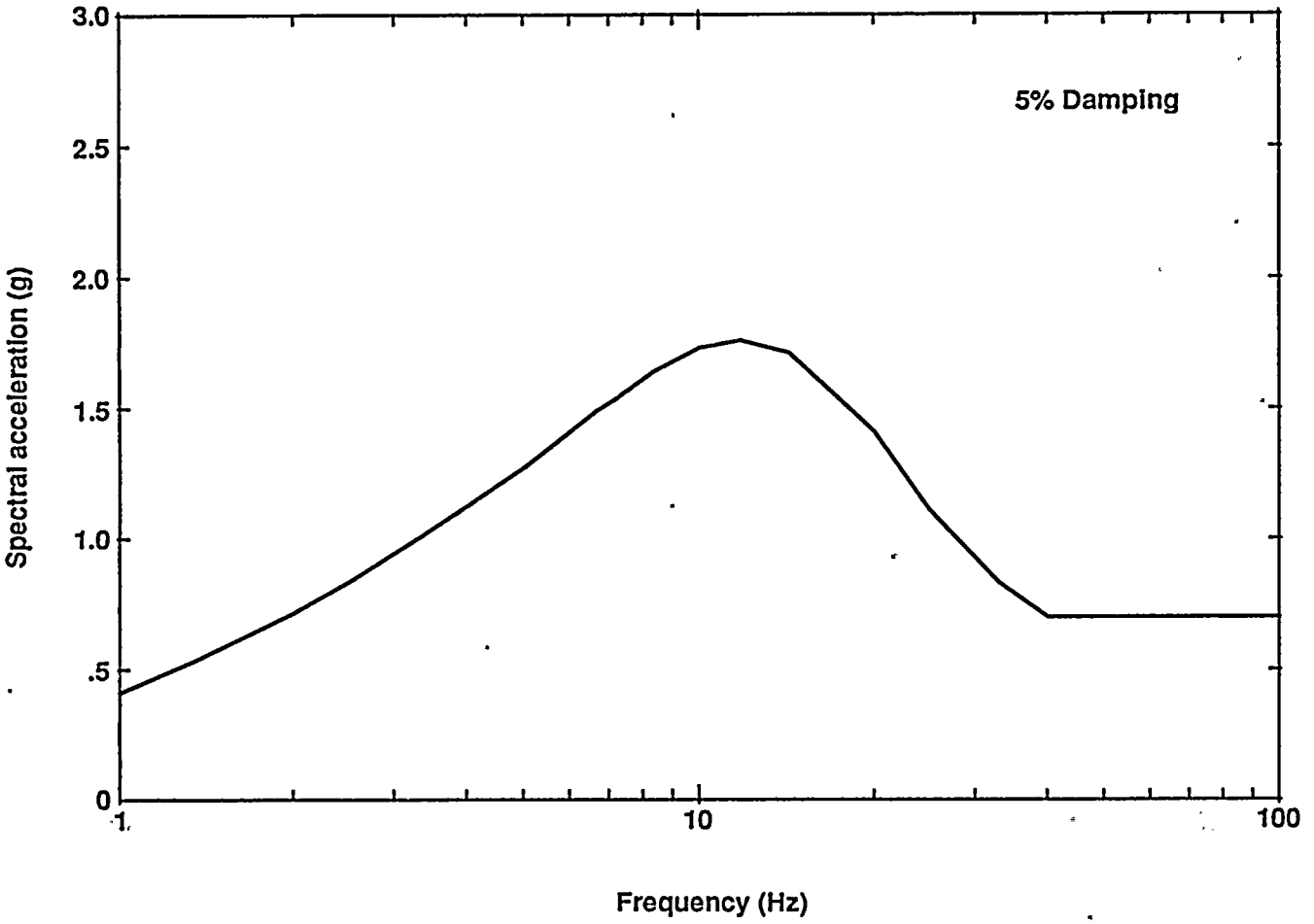

Figure DE Q2-2

84th-percentile, site-specific vertical ground motion response spectrum for the maximum magnitude earthquake.

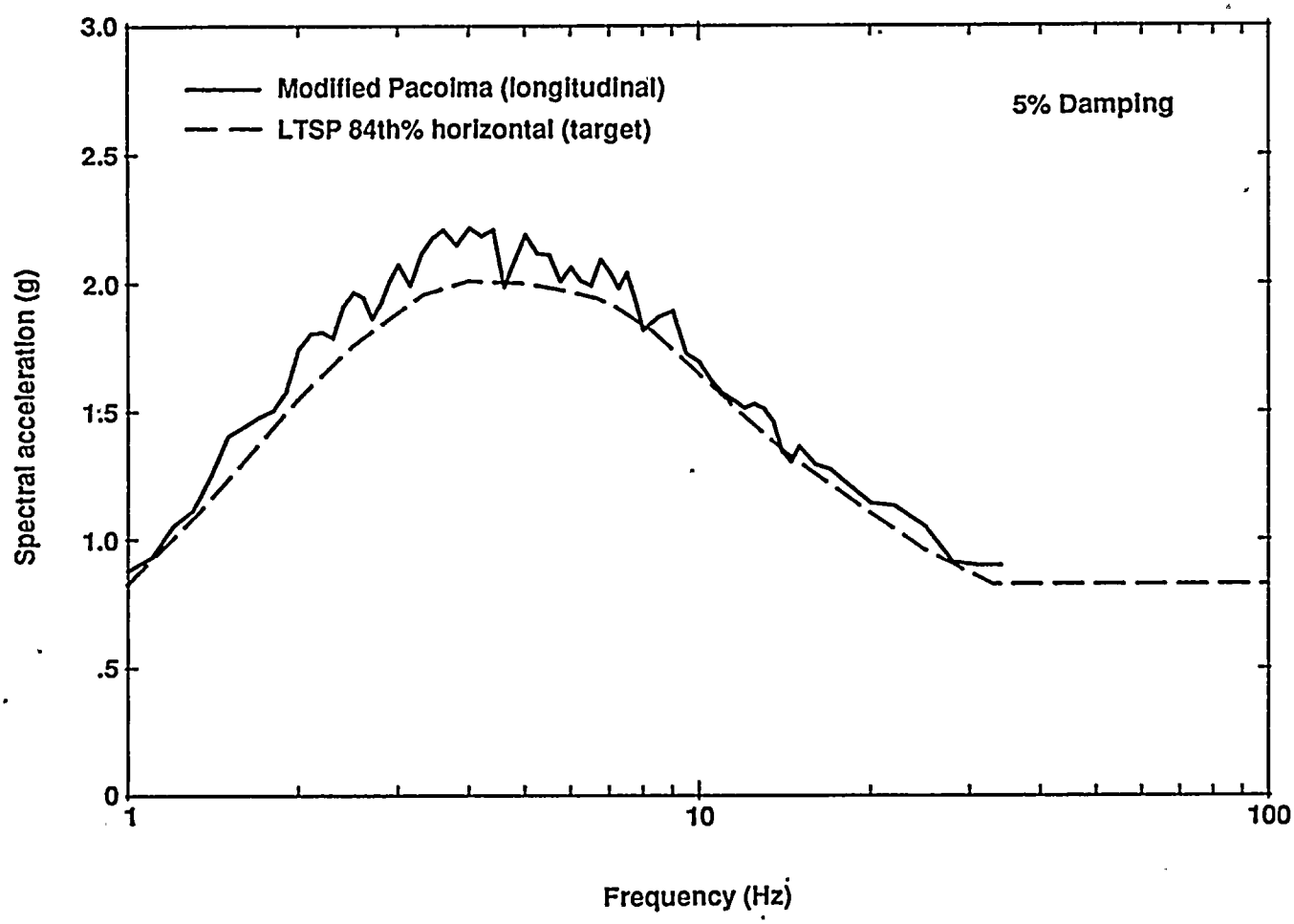

Figure DE Q2-3

Comparison of the modified Pacoima time-history response spectrum with the 84th-percentile, site-specific horizontal ground motion response spectrum, longitudinal component.

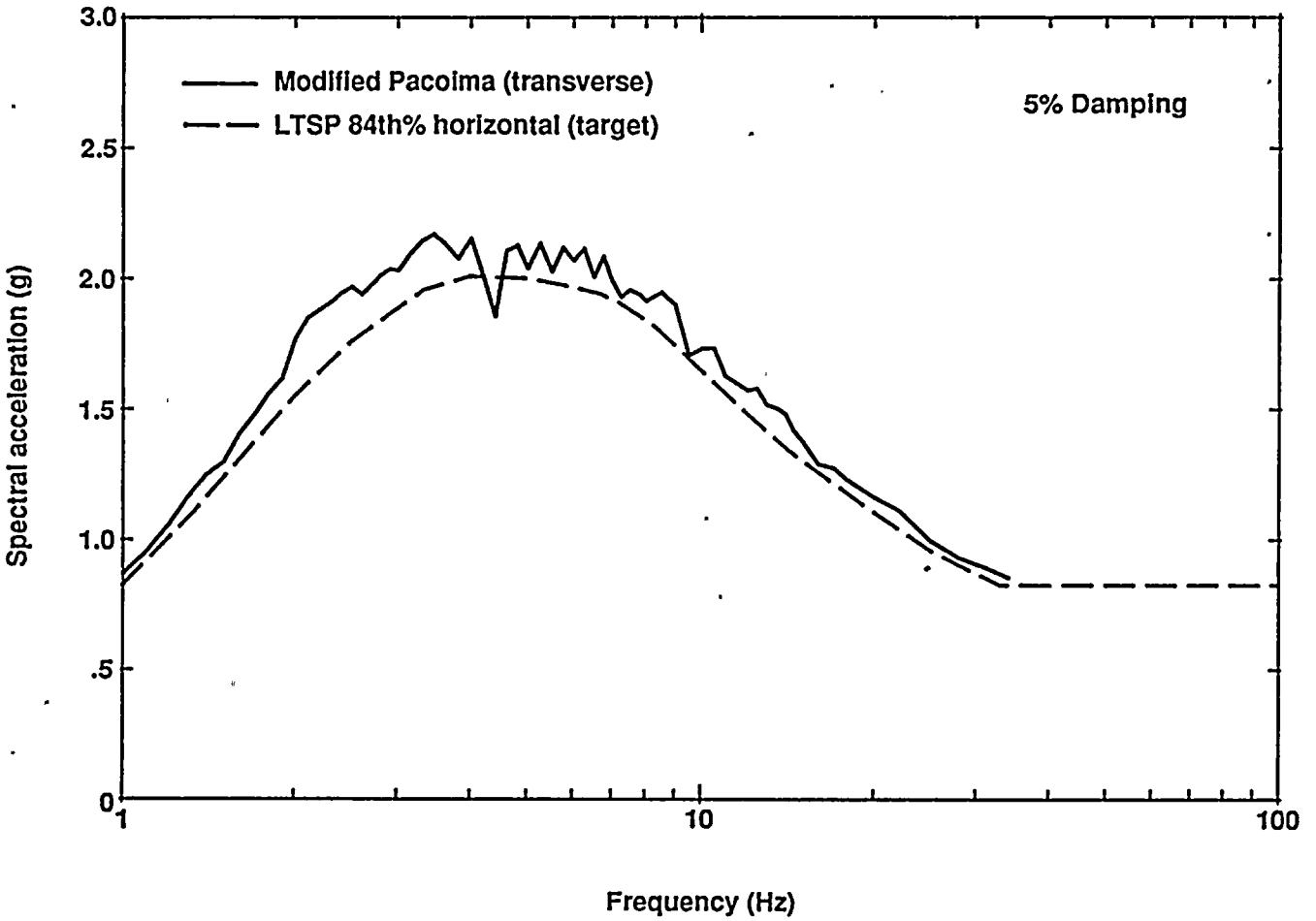

Figure DE Q2-4

Comparison of the modified Pacoima time-history response spectrum with the 84th-percentile, site-specific horizontal ground motion response spectrum, transverse component.

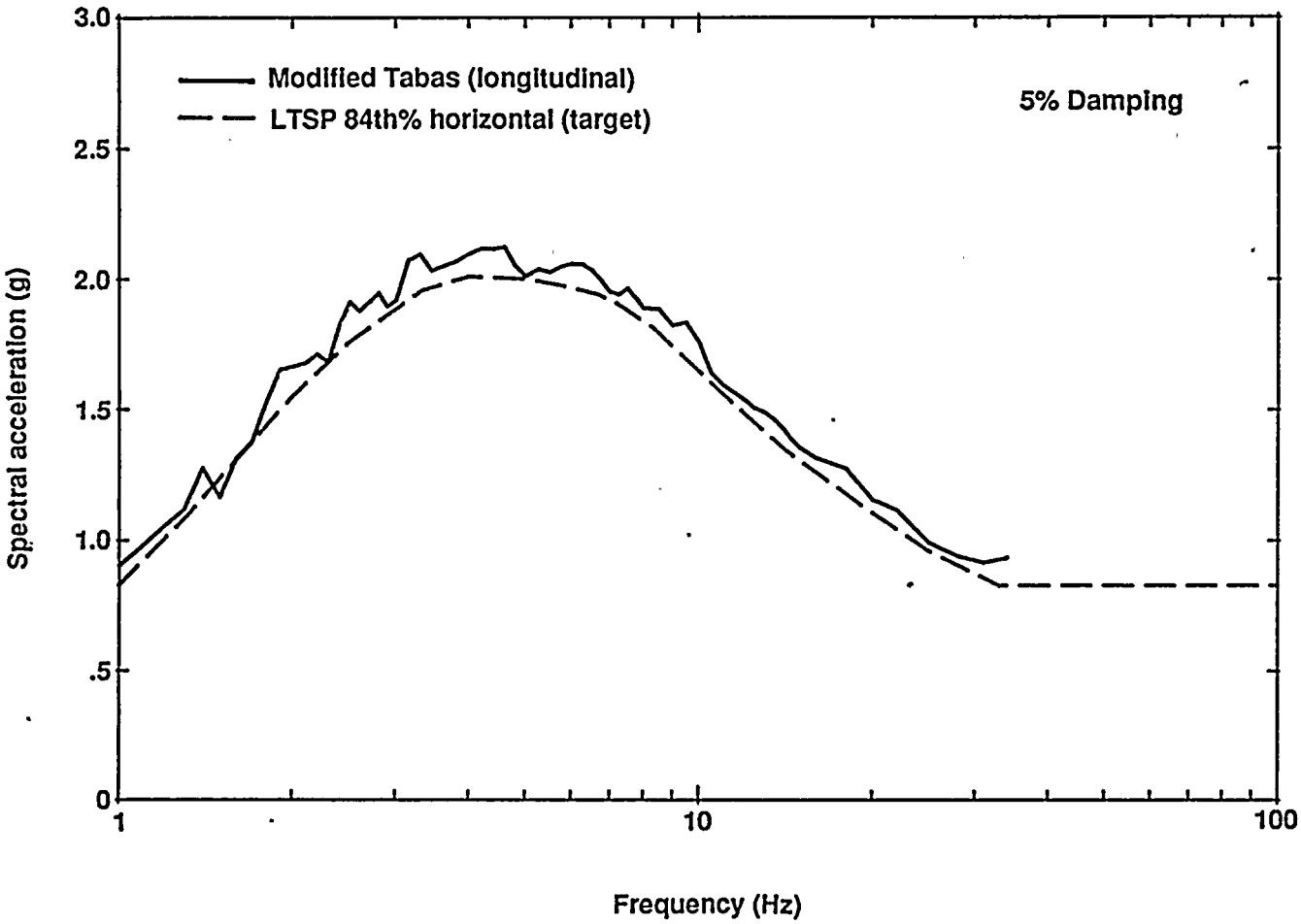

Figure DE Q2-5

Comparison of the modified Tabas time-history response spectrum with the 84th-percentile, site-specific horizontal ground motion response spectrum, longitudinal component.

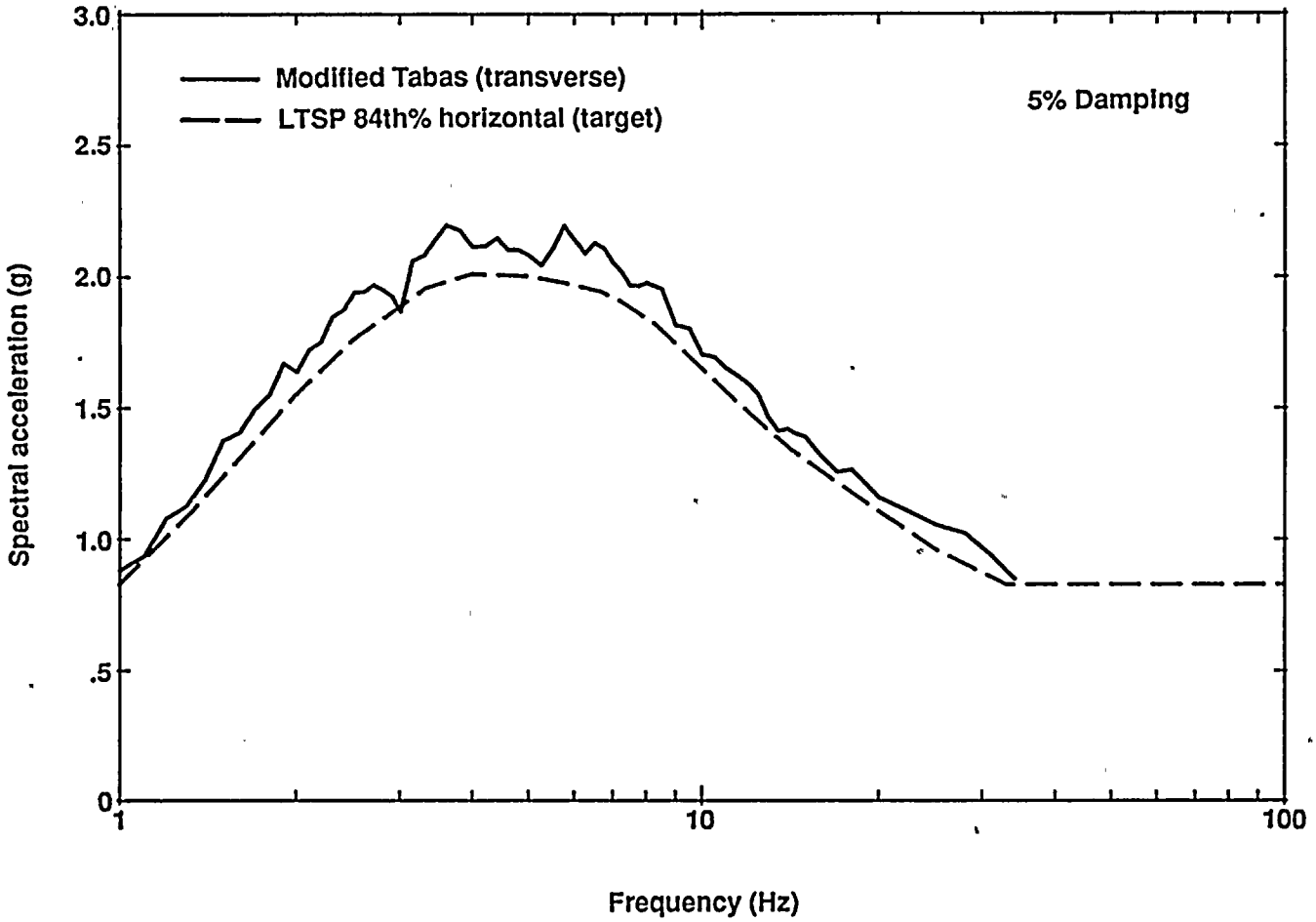

Figure DE Q2-6

Comparison of the modified Tabas time-history response spectrum with the 84th-percentile, site-specific horizontal ground motion response spectrum, transverse component.

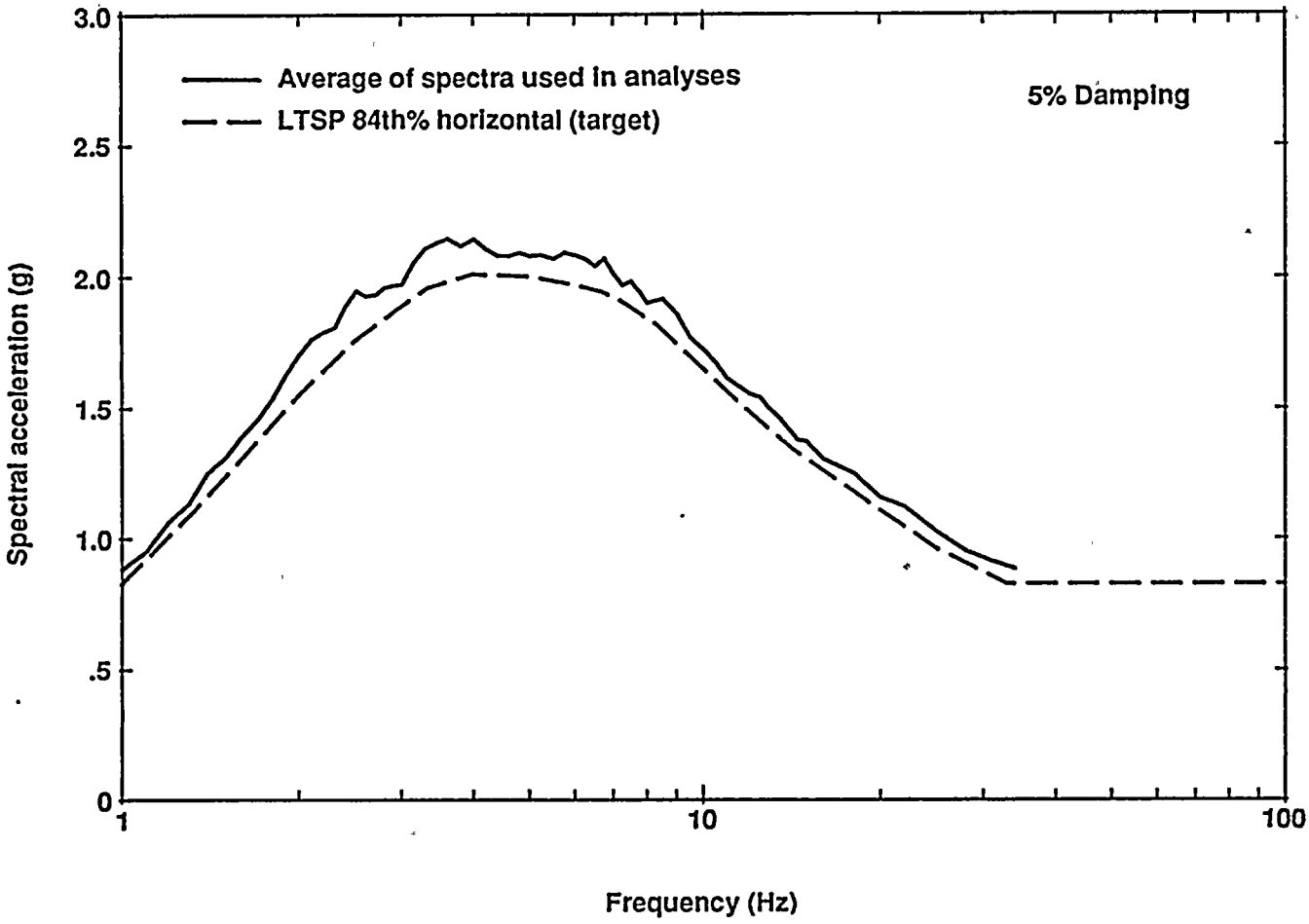

Figure DE Q2-7

Comparison of the average modified Pacoima and Tabas time-history horizontal response spectrum with the 84th-percentile, site-specific horizontal ground motion response spectrum.

QUESTION DE 3

Describe the procedure that was used to calculate seismic response loads (demands) on the Plant structures.

The procedure described in Chapter 5 of the Diablo Canyon Long Term Seismic Program Final Report (PG&E, 1988) was followed to calculate the seismic responses of the containment, auxiliary, and turbine buildings. The SASSI computer program was used for soil/structure interaction analysis of these structures using the same three-dimensional dynamic models as described in PG&E, 1988. The soil/structure interaction effects are more significant for the horizontal responses than for the vertical response. The analyses were thus performed for the horizontal north-south and east-west ground motion inputs only. The coupling between the two horizontal responses that exists for nonsymmetrical structures was considered by combining the co-directional time-history responses. The modified Pacoima and Tabas time-histories, which are compatible with the site-specific response spectrum, were prescribed on the ground surface at the finished grade of the Plant (elevation 85 feet). The free-field seismic incidence wave field was considered as vertically propagating plane seismic shear waves polarized in the Plant north-south and east-west directions for the horizontal north-south and east-west inputs, respectively. Under the vertically propagating plane wave assumption, the contributions to the horizontal responses due to the vertical input motion are negligible.

As described in PG&E, 1989, the vertical responses for the 84th-percentile ground motion were obtained by multiplying the vertical responses that were used for the Hosgri reevaluation by the ratio of the 5 percent damped 84th-percentile vertical ground spectrum to the 5 percent damped Hosgri reevaluation vertical ground spectrum.

For each time-history input case corresponding to the two horizontal directions of the modified Pacoima and Tabas records, the time-history response of the global seismic load of interest (e.g., the shear force or overturning moment for a particular structural element in the dynamic model) was calculated using SASSI, and the maximum time-history response was obtained. The maximum values from all four time-history input cases were then averaged to obtain the final maximum value of the seismic load of interest for the particular seismic input direction considered. The maximum co-directional response values due to the two horizontal inputs, namely, the north-south and east-west inputs, were combined using the square-root-of-the-sum-of-squares or the 1 + 0.4 + 0.4 combination rule. As discussed in Question DE 2, the exceedance of the artificial time-history average response spectrum over the 84th-percentile, site-specific horizontal response spectrum was more than 5 percent. The seismic loads were, therefore, reduced by 5 percent to remove this conservatism.

Since the containment shell and internal structures were represented by two separate sticks in the dynamic model, the global seismic base shear force and overturning moment were obtained directly from responses of the two sticks. However, for the auxiliary building, the maximum seismic shear forces and overturning moments for the entire structure were obtained by combining the responses of the individual sticks of the 5-stick dynamic model. The turbine building was modeled with a three-dimensional, finite element model and direct determination of seismic shear forces and overturning moments was not practical. In this case, the time-history stresses in the individual finite elements of the major load resisting elements were appropriately integrated over the length of the walls to give the time-history of shear forces. The moments were obtained from the shear diagram.

ADJUSTMENT FOR SPATIAL INCOHERENCY OF GROUND MOTION

The seismic response quantities obtained for the Plant structures for coherent ground motion inputs were adjusted to account for spatial incoherency effects. These adjustments were based on the ratios of zero-period acceleration responses to incoherent and coherent ground motions at different floor levels. The adjustment factors were the same as those presented in Chapter 5 of PG&E, 1988. The difference of seismic shear forces above and below a particular floor level represented the seismic inertial load at that floor. The inertia load thus obtained was adjusted to account for the spatial incoherency effect at the respective floor levels. The seismic shear force distribution was determined by progressively following this procedure from the top of the structure to the base. The overturning moments were calculated from these adjusted story shears.

REFERENCES

Pacific Gas and Electric Company, 1988, Final report of the Diablo Canyon Long Term Seismic Program: U. S. Nuclear Regulatory Commission, Docket Nos. 50-275 and 50-323.

Pacific Gas and Electric Company, 1989, letter No. DCL-89-022, Response to NRC staff questions on the Long Term Seismic Program (Question 1).

QUESTION DE 4

Compare the seismic base shear and overturning moments in the containment, auxiliary, and turbine buildings due to the maximum magnitude earthquake with the corresponding seismic responses determined using the Hosgri reevaluation criteria. The comparisons should be provided for the global structure and for selected structural elements in each building.

Figure DE Q4-1 shows the configuration of the Plant power block structures. The figure also identifies the structural elements in the auxiliary and turbine buildings for which additional deterministic evaluations were performed. The structural elements examined for the containment building were the exterior shell and the concrete interior structure, which includes the crane wall and the reactor shield wall. As shown in Figure DE Q4-2, these structural elements are cylindrical, reinforced concrete walls supported on a common basemat at elevation 89 feet. While there are several walls that comprise the concrete interior structures, the crane wall and the reactor shield wall are the major lateral force resisting elements. Table DE Q4-1 shows the shear forces, overturning moments, and torsional moments at the base of the containment shell and the interior structure for the 84th-percentile ground motion for the maximum magnitude earthquake and the Hosgri reevaluation. The forces and moments at elevation 172 feet of the containment shell are also provided. The inclined reinforcing bars near the inner face of the shell terminate at this location. Table DE Q4-1 also includes Hosgri shear force and moment capacities of the containment shell and interior structure.

The maximum magnitude earthquake shear and moment demands for the containment building exceed the Hosgri demands at the sections evaluated, but the maximum magnitude earthquake torsional moments are significantly less than the Hosgri torsional moments. Table Q4-1, however, shows that the maximum magnitude earthquake demands remain below the Hosgri capacities at the containment shell and interior structure sections. Also, the response to Question DE 6 shows that the maximum magnitude earthquake demands can be accommodated by the capacities of these structural elements with substantial margin.

Table DE Q4-2 shows the shear forces and moments at the base and elevation 100 feet of the auxiliary building due to the maximum magnitude earthquake and the Hosgri reevaluation. The table shows seismic demand forces only. The table shows the global loads on the building and the local loads in the shear walls at lines 6.4, 15.7, 20.3, 29.6, and H (Figure DE Q4-1). These walls were selected for evaluation because they were identified as providing the controlling failure modes for the building fragility analysis or were determined to be the critical walls during the Hosgri reevaluation. The maximum magnitude earthquake loads compare well with those obtained from the Hosgri reevaluation. The response to Question DE 6 shows that the maximum magnitude earthquake demands can be accommodated by the capacities of these structural elements with substantial margin.

The turbine building shear walls at column lines 17, 19, 31, and G (Figure DE Q4-1) were evaluated. Wall 17 is the most critical east-west shear wall of Unit 1. Walls 19 and 31 are the two major shear walls of Unit 2 in the east-west direction. Wall G is one of the two north-south shear walls of the structure and was identified as the critical north-south wall for the Hosgri reevaluation. Table DE Q4-3 shows the shear forces and moments at selected sections of these walls for the maximum magnitude earthquake and the Hosgri reevaluation. The table shows seismic demand forces only. In general, the maximum magnitude earthquake demands are higher than the Hosgri demands. The response to Question DE 6 shows that the maximum magnitude earthquake demands can be accommodated by the capacities

of these structural elements with substantial margin.

It should be noted that the objective of the Plant qualification evaluations for design and licensing purposes, including the reevaluation for the Hosgri earthquake, was to demonstrate that structures meet or exceed specified criteria, and not to quantify seismic margins. The Plant seismic qualification basis methods contained numerous conservatisms. Different strength evaluation methods were used for the evaluation of different buildings consistent with licensing criteria. For example, the evaluation of shear walls in the turbine building was performed using Structural Engineers Association of California (1974) strength equations; those of the auxiliary building were performed using a set of project-specific criteria. Thus, comparison of maximum magnitude earthquake demands and Hosgri demands and Hosgri capacities, while of interest, cannot and should not be used as a basis for determining seismic margins.

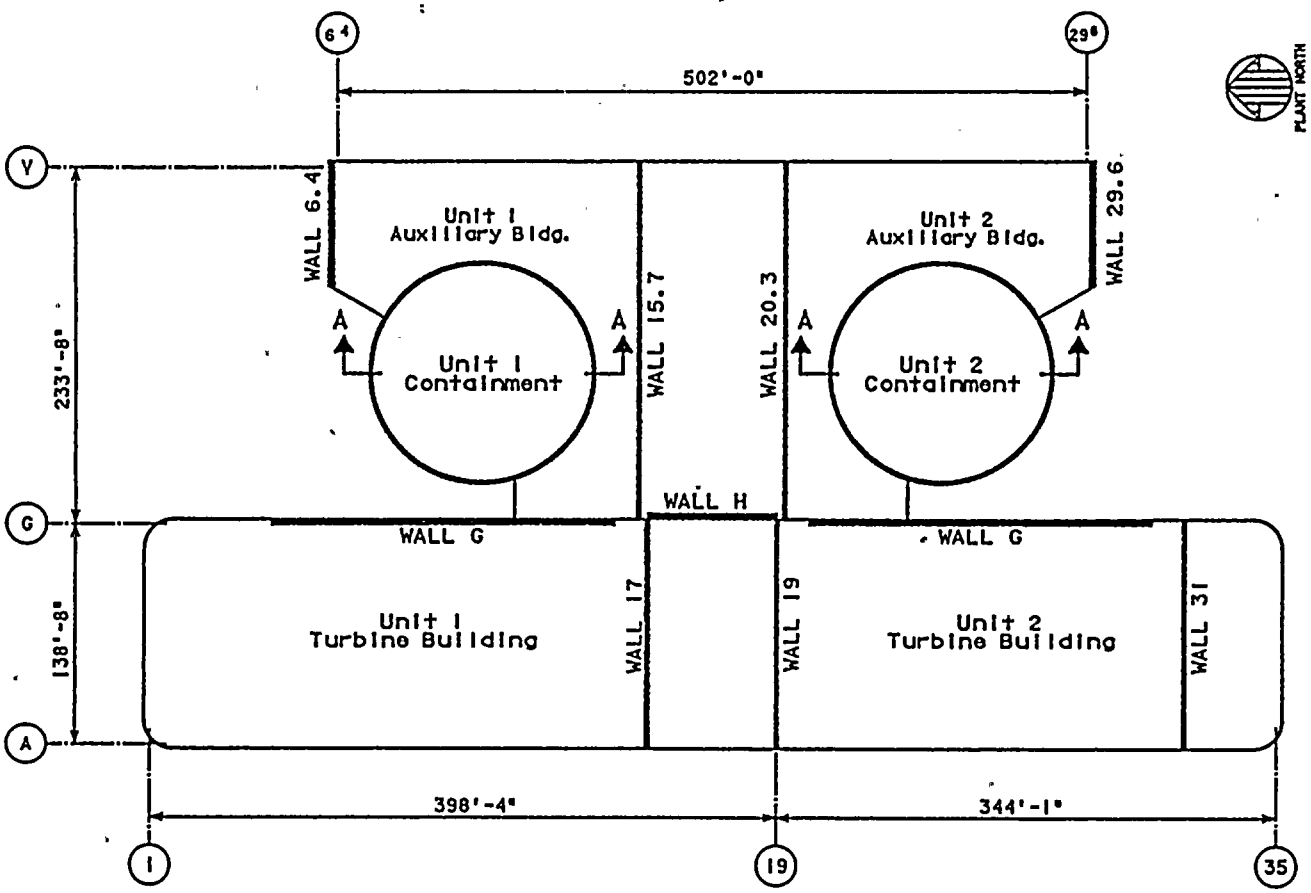

Figure DE Q4-1

Plant power block structures and structural elements selected for evaluation by the conservative deterministic failure margin approach.

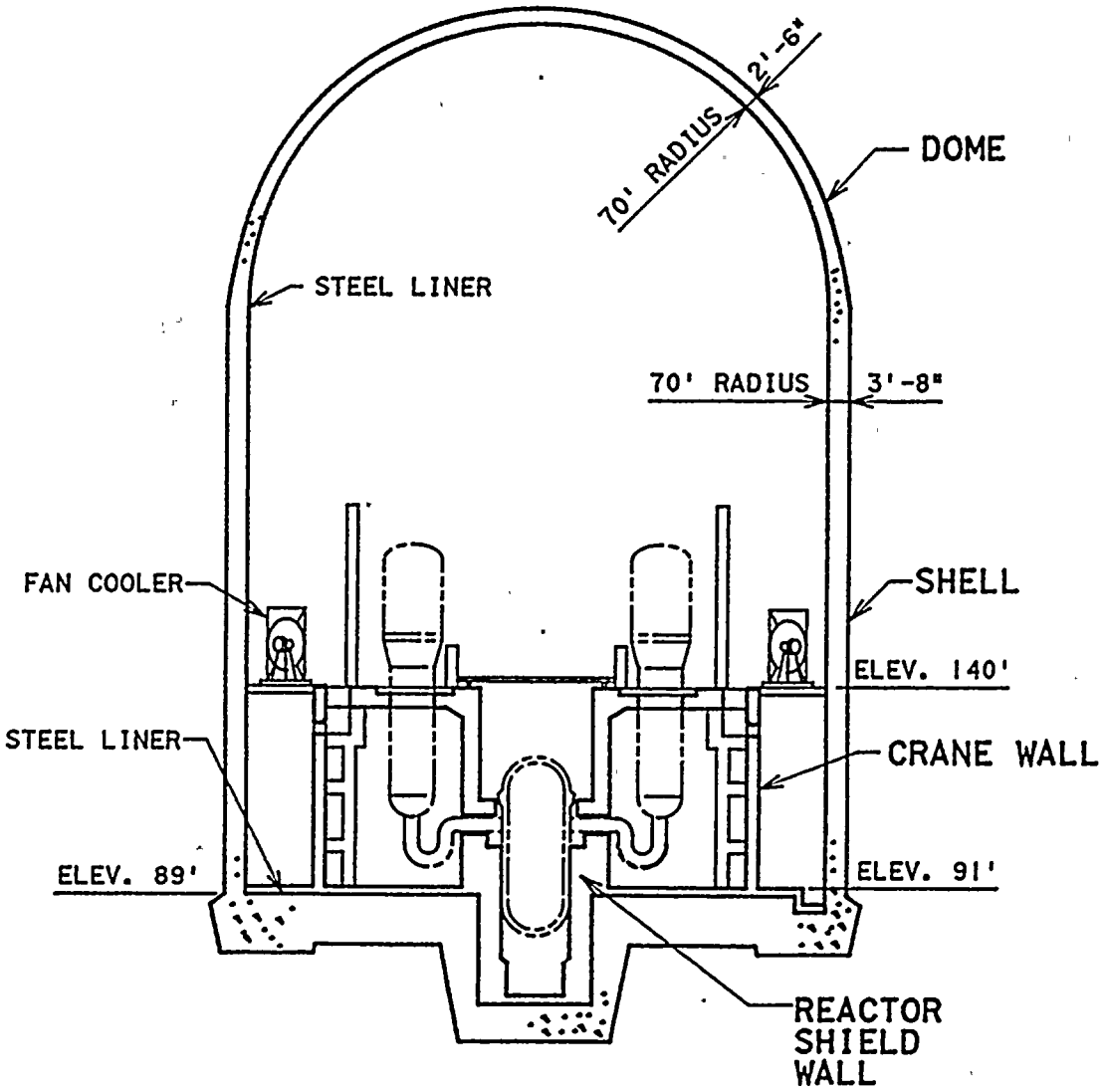

Section A-A
(Figure DE Q4-1)

Figure DE Q4-2

Containment shell and concrete interior structures evaluated by the conservative deterministic failure margin approach.

Table DE Q4-1

CONTAINMENT STRUCTURE

COMPARISON OF MAXIMUM MAGNITUDE EARTHQUAKE AND HOSGRI EARTHQUAKE DEMANDS AND CAPACITIES

Wall Location	Elev (ft)	Shear (kips x 10^3) MME Demand	Shear (kips x 10^3) Hosgri Demand	Shear (kips x 10^3) Hosgri Capacity	Moment (ft-kips x 10^3) MME Demand	Moment (ft-kips x 10^3) Hosgri Demand	Moment (ft-kips x 10^3) Hosgri Capacity	Torsion (ft-kips x 10^3) MME Demand	Torsion (ft-kips x 10^3) Hosgri Demand
Shell	172	62.1	45.4	83	4,240	3,400	10,000	none	400
	89	80.1	55.8	120	9,800	7,310	18,000	none	440
Interior Structure	91	37.6	24.1	51	1,490	790	2,470	94.5	284

Table DE Q4-2

AUXILIARY BUILDING

COMPARISON OF MAXIMUM MAGNITUDE EARTHQUAKE AND HOSGRI EARTHQUAKE DEMANDS

Wall Location Col Line		Elev (ft)	Shear (kips x 10^3) MME	Shear (kips x 10^3) Hosgri	Moment (ft-kips x 10^3) MME	Moment (ft-kips x 10^3) Hosgri
H		100	10.1	10.3	219	176
		85	10.6	11.3	335	270
15.7 or 20.3		85	25.0	21.9	851	669
6.4 or 29.6		100	8.1	8.9	245	269
Auxiliary Building, Global	N-S	100	141	120	4,990	4,140
		85	107	104	4,980	5,700
	E-W	100	137	128	5,190	4,410
		85	101	102	4,600	5,940

Table DE Q4-3

TURBINE BUILDING WALLS

COMPARISON OF MAXIMUM MAGNITUDE EARTHQUAKE AND HOSGRI EARTHQUAKE DEMANDS

Unit No.	Wall Location Col Line	Elev (ft)	Shear (kips x 10^3) MME	Shear (kips x 10^3) Hosgri	Moment (ft-kips x 10^3) MME	Moment (ft-kips x 10^3) Hosgri
2	19	104	7.8	7.7	295	287
		85	9.4	7.7	459	422
2	31	119	10.9	7.8	229	164
		85	11.8	8.1	590	440
2	G	104	12.3	10.4	360	336
		85	18.4	13.2	703	580
1	17	104	9.1	8.8	345	320
		85	11.0	9.1	537	479
1	G	104	12.9	11.8	378	366
		85	19.3	13.8	738	629

QUESTION DE 5

Compare the seismic base shear and overturning moments in the containment, auxiliary, and turbine buildings due to the maximum magnitude earthquake with the corresponding capacities determined using Hosgri reevaluation criteria.

Maximum magnitude earthquake loads on selected building structural elements were compared with the capacities of those elements that were determined using Hosgri reevaluation criteria. For these comparisons, capacities were derived considering the loads to be the Hosgri seismic loads combined with the other applicable loads. For example, containment structure capacities were derived considering the presence of a concurrent accident pressure resulting from a large-break loss-of-coolant-accident.

The containment building seismic loads from the maximum magnitude earthquake are compared with the Hosgri capacities in Table DE Q5-1. The capacities of the containment shell and the interior structure were not explicitly calculated during the Hosgri reevaluation since the objective of the reevaluation was only to show that specified criteria were met. Instead, during the Hosgri reevaluation, stresses resulting from the governing load combination were derived and compared to the Hosgri acceptance criteria. For the purpose of this evaluation, however, the Hosgri capacities have been calculated for the exterior shell and the interior structure on the basis of Hosgri acceptance criteria.

The auxiliary building seismic loads from the maximum magnitude earthquake are compared with Hosgri capacities in Table DE Q5-2. Table DE Q5-3 provides a similar comparison for the selected turbine building walls. The response to Question DE 6 shows that the increases in demands in the turbine building walls due to maximum magnitude earthquake loads can be accommodated by the structural capacities with ample margin.

Comparison of maximum magnitude earthquake demands with Hosgri capacities should not be used as a basis to determine seismic margin (see Question DE 4, page 2). Seismic margins are quantified in Tables DE Q6-1, DE Q6-2, and DE Q6-3.

Table DE Q5-1

CONTAINMENT BUILDING

COMPARISON OF MAXIMUM MAGNITUDE EARTHQUAKE DEMANDS AND HOSGRI EARTHQUAKE CAPACITIES[1]

Wall Location	Elev (ft)	Shear (kips x 10^3)		Moment (ft-kips x 10^3)	
		MME Demand	Hosgri Capacity	MME Demand	Hosgri Capacity
Shell	172	62.1	83	4,240	10,000
	89	80.1	120	9,800	18,000
Interior Structure	91	37.6	51	1,490	2,470

NOTE:

1 Comparison of maximum magnitude earthquake demands with Hosgri capacities should not be used as a basis to determine seismic margin (see Question DE 4, page 2). Seismic margins are quantified in Table DE Q6-1.

Table DE Q5-2

AUXILIARY BUILDING WALLS

COMPARISON OF MAXIMUM MAGNITUDE EARTHQUAKE DEMANDS AND HOSGRI EARTHQUAKE CAPACITIES[1]

Wall Location Col Line	Elev (ft)	Shear (kips x 10^3)		Moment (ft-kips x 10^3)	
		MME Demand	Hosgri Capacity	MME Demand	Hosgri Capacity
H	100	10.1	12.4	219	504
	85	10.6	14.2	335	682
15.7 or 20.3	85	25.0	29.8	851	1,460
6.4 or 29.6	100	8.1	10.2	245	434

NOTE:

[1] Comparison of maximum magnitude earthquake demands with Hosgri capacities should not be used as a basis to determine seismic margin (see Question DE 4, page 2). Seismic margins are quantified in Table DE Q6-2.

Table DE Q5-3

TURBINE BUILDING WALLS

COMPARISON OF MAXIMUM MAGNITUDE EARTHQUAKE DEMANDS AND HOSGRI EARTHQUAKE CAPACITIES[1]

Unit No.	Wall Location Col Line	Elev (ft)	Shear (kips x 10^3)		Moment (ft-kips x 10^3)	
			MME Demand	Hosgri Capacity	MME Demand	Hosgri Capacity
2	19	104	7.8	9.9	295	402
		85	9.4	9.1	459	704
2	31	119	10.9	11.0	229	495
		85	11.8	10.1	590	983
2	G	104	12.3	18.0	360	780
		85	18.4	18.7	703	1,140
1	17	104	9.1	9.9	345	422
		85	11.0	10.2	537	612
1	G	104	12.9	18.0	378	780
		85	19.3	18.7	738	1,070

NOTE:

[1] Comparison of maximum magnitude earthquake demands with Hosgri capacities should not be used as a basis to determine seismic margin (see Question DE 4, page 2). Seismic margins are quantified in Table DE Q6-3.

QUESTION DE 6

Evaluate the capacities of structural elements using the conservative deterministic failure margin (CDFM) approach. Compare the loads in the structural elements due to the maximum magnitude earthquake with the corresponding CDFM capacities. Establish the seismic margins in the structural elements selected for evaluation.

The conservative deterministic failure margin approach developed under the sponsorship of Electric Power Research Institute (EPRI, 1988) is described in Attachment DE Q6-A. The attachment includes discussions of how the EPRI recommendations were adopted for the Diablo Canyon additional deterministic evaluations, or the basis for an alternate approach in a few cases.

CONTAINMENT BUILDING

Containment Shell

The shear and flexural capacities of the containment shell were evaluated at the base of the building at elevation 89 feet, where the seismic forces are the greatest, and at elevation 172 feet where the inner curtain of diagonal reinforcing steel terminates. In evaluating the shear capacity, the containment shell was treated as a thin-walled, reinforced concrete cylinder and the strength equations described in Attachment DE Q6-A (Equations 9 - 11) were used. The horizontal shear resistance is provided by the concrete, the hoop reinforcing, and the diagonal bars. Since the strength equation is based on the reinforcing ratios in the hoop and meridional directions, the components of the areas of the diagonal bars in the hoop and meridional directions were used to calculate the effective reinforcement ratios. To provide additional conservatism, the liner was not included in the shear capacity evaluation because of the potential for local buckling when the liner is subjected to the horizontal shear forces.

The flexural capacity evaluation was based on the ultimate flexural strength provisions prescribed by the ACI Code. The flexural resistance is provided by the concrete, the diagonal bars, and the liner. The components of the diagonal bars in the meridional direction were used in the flexural strength calculation. The liner was not considered to be effective in carrying compressive bending stress, again due to the potential for plate buckling. However, because the anchorage of the liner to the containment wall is sufficient to develop the required strain compatibility between the liner and the concrete, the liner was considered to be effective in carrying tensile bending stress.

The shear and flexural capacities of the containment shell were evaluated at elevations 89 feet and 172 feet both with and without an internal pressure of 22 psi due to a small-break LOCA, as opposed to an accident pressure of 47 psi that was used for the Hosgri reevaluation. In the case of shear capacity, the pressure adds tensile membrane stresses in the hoop and meridional directions of the shell. This has the effect of reducing the effective steel ratio and thus, the capacity. For the flexural capacity, the internal pressure has the effect of adding a net tensile axial load to the cross-section. This also reduces the overall capacity.

Containment Interior Structures

The shear capacity of the interior structure was evaluated as the global shear capacity, derived as the sum of the shear capacities of all the contributing walls at the base. The evaluation considered that the fuel

canal walls and bottom slab and the elevation 140 feet floor are capable of redistributing shear forces to all the contributing walls. Shear capacities were evaluated as described in Attachment DE Q6-A. The shield wall was treated as a thick-walled cylinder (Equations 12-15). The crane wall was treated as a thin-walled cylinder (Equations 9-11), and the other walls were treated as planar shear walls (Equations 7 and 8). The shield wall cross-section at elevation 91 feet was conservatively considered to be the reduced cross-section at elevation 107 feet where reactor coolant piping penetrates the wall.

The flexural capacity of the interior structures is dependent on the direction of the horizontal earthquake motion. In the east-west direction, the fuel canal walls, as well as other walls and slabs, interconnect the shield and crane walls so that they act together as a composite system to resist overturning moments. However, in the controlling direction (north-south), there is no shear wall interconnecting the shield and crane walls (Figure DE Q4-2). Thus, no mechanism exists to enable the shield and crane walls to act as a composite system to resist overturning. Accordingly, flexural capacities of the shield and crane walls were evaluated separately using a method similar to that described for concrete shear walls in Attachment DE Q6-A (Equation 6).

Evaluation of Capacities and Margin

Different concrete mixes were specified for the containment building shell and the interior structures. The concrete compressive strengths were established using the relations described in Attachment DE Q6-A (Equation 1). For the exterior shell, a Type B concrete mix was used with a specified minimum 28-day compressive strength of 3,000 psi. The average tested strength was 3,850 psi. As a result, the 95 percent probability of exceedance strength value used in the CDFM capacity evaluation for the exterior shell was 3,650 psi. For the interior structures, a Type A concrete mix was used with a specified minimum 60-day compressive strength of 5,000 psi and an average tested strength of 6,330 psi. For the Type A mix, the CDFM concrete compressive strength was taken as 5,820 psi.

The steel yield strength was taken as the code specified minimum value. In both the containment shell and the interior structures, Grade 60 reinforcing bars were specified and the CDFM yield strength for the reinforcing was taken as 60 ksi. The liner plate for the containment shell is fabricated from ASME SA-516 Grade 70 steel plate, having a code minimum yield strength of 38 ksi. Thus, the yield stress for the liner plate was taken as 38 ksi.

A conservative inelastic energy absorption factor, F_μ (Equations 16 and 17 of Attachment DE Q6-A), of 1.25 was used in the evaluation of the containment shell and interior structures. As discussed in Attachment DE Q6-A, a value exceeding 1.25 could be determined from more rigorous analysis.

The maximum magnitude earthquake demands on the containment shell and the selected interior walls are compared to the corresponding CDFM capacities in Table DE Q6-1. The seismic margins are reported in terms of the scale factor FS_I defined in Attachment DE Q6-A (Equation 24).

The critical failure modes for the containment building were determined to be shear failure of the exterior cylindrical shell at the base and flexural failure of the shield wall at the base. The minimum scale factor, FS_I, was calculated to be 1.79.

AUXILIARY BUILDING

As discussed in response to Question DE 4, the auxiliary building shear walls at lines 6.4, 15.7, 20.3, 29.6, and H were selected for evaluation because these walls were identified as the controlling failure

modes for the building fragility analysis or were identified as the critical walls during the Hosgri reevaluation. The conservative deterministic failure capacities of these walls were evaluated using the approach described in Attachment DE Q6-A (Equations 6 - 8).

Shear walls in the auxiliary building are typically squat (height/length ratio less than 1), lightly reinforced (reinforcement ratio less than 1 percent) shear panels, with a thickness of at least 24 inches. Reinforced concrete floor diaphragms at elevations 85, 100, 115, 140, 154, and 163 feet typically connect these shear walls.

The compressive strength of concrete (f_c') was computed from the median compressive strength at 28 days (based on cylinder tests specific to the auxiliary building), an aging factor, and the corresponding variabilities, as described in Attachment DE Q6-A (Equation 1). For the auxiliary building, an f_c' value of 5,300 psi, corresponding to a minimum specified value of 5,000 psi, was used.

The yield strength of reinforcing steel in the deterministic evaluation was conservatively taken as the ASTM-specified minimum value. For the auxiliary building, ASTM A615 Grade 40 (f_y = 40,000 psi) or Grade 60 (f_y = 60,000 psi) reinforcing steel was used.

For simplicity, a conservative inelastic energy absorption factor, F_μ, of 1.25 was used for the auxiliary building shear walls. As noted in Attachment DE Q6-A, a value exceeding 1.25 could be determined from more rigorous analysis.

The maximum magnitude earthquake demands on the auxiliary building walls are compared to the corresponding CDFM capacities in Table DE Q6-2. The table also shows seismic margins of the walls in terms of the scale factor FS_l. This factor is defined in Attachment DE Q6-A (Equation 24). Results are given for each wall evaluated and also for the governing group of walls in the north-south and east-west directions.

The capacities and margins for the individual walls, although of interest, are not a realistic measure of the seismic margin of the building because they do not account for the capability of the building to redistribute forces. The building lateral force resisting system consists of floor diaphragm slabs connected to numerous shear walls extending in both the north-south and east-west directions. Because of the high capacity of the floor diaphragms and the redundancy of the system, an individual wall that has reached its elastic capacity does not lead to failure of the building. Instead, the wall will yield, and additional load will be distributed to adjacent walls which have not yet reached their capacities. Reserve capacity is available not only in walls parallel to the direction of the principal earthquake component, but also in walls perpendicular to that direction (cross-walls). The cross-walls have substantial reserve capacity to resist the torsional moment because the maximum value of earthquake components in the north-south and east-west directions are not considered to be concurrent.

The CDFM capacities shown in Table DE Q6-2 for the group of north-south walls located in the western core of the building, and for the group of east-west walls in the main core of the building, include the effects of redistribution. For the north-south direction, the building capacity is governed by the group of walls at lines H, J, and K. The scale factor, FS_l, for this group of walls was computed as the ratio of their total capacity to their total demand considering redistrubution of both translation-induced and torsion-induced forces. In the east-west direction, the building capacity is governed by the pair of walls at lines 15.7 and 20.3. The scale factor for these walls was computed similarly, considering only the redistribution of torsion-induced forces to the cross-walls.

The controlling group of auxiliary building walls was determined to be the pair of walls at lines 15.7 and 20.3 with a scale factor of 1.76.

TURBINE BUILDING

As discussed in response to Question DE 4, the turbine building major shear walls at lines G and 17 in Unit 1 and lines G, 19, and 31 in Unit 2 were selected for evaluation because these walls were identified as the controlling failure modes for the building fragility analysis or were identified as critical walls during the Hosgri reevaluation. The CDFM capacities of these walls were evaluated using the approach described in Attachment DE Q6-A (Equations 6 - 8).

Shear walls in the turbine building are also typically squat (height/length ratio less than 1), lightly reinforced (reinforcement ratio less than 1 percent) shear panels, with a thickness of from 16 to 38 inches. Steel plate floor diaphragms or integrally constructed reinforced concrete floor diaphragms are connected to the shear walls at elevations 140, 119, and 104 feet. Structural steel wide flange columns and beams located at the main floor levels and embedded in the shear walls are characteristic of each of the major shear walls of the building. Horizontal and vertical wall reinforcing steel passes through these embedded structural steel members and provides continuity.

The flexural reinforcement yield failure mode capacity of the walls was calculated, in most cases, by including the yield force capacity associated with the embedded structural steel columns. At the base of the wall, the yield force capacity of the column is limited by its anchor bolts (yielding of ASTM A307 steel bolts). At sections above the base of the wall, a larger capacity can be developed because of column embedment and the presence of additional vertical reinforcement in the lowest story of the wall.

The compressive strength of concrete (f_c') was computed from the median compressive strength at 28 days (based upon cylinder tests specific to the turbine building), an aging factor, and the corresponding variabilities, as described in Attachment DE Q6-A. Because of modifications to reinforced concrete shear walls performed following the Hosgri reevaluation, statistical data from two phases of construction were used. The f_c' values used are 5,240 to 5,400 psi, and 3,700 psi, corresponding to minimum specified values of 5,000 psi and 3,000 psi, respectively.

The yield strength of reinforcing steel was conservatively taken as the ASTM-specified minimum value. These are 40,000 psi for ASTM A615 Grade 40 and 60,000 psi for Grade 60 reinforcing bars. The yield strength of structural steel members was taken as the ASTM specified minimum value for ASTM A36 (F_y = 36,000 psi).

For shear walls in the turbine building, an inelastic energy absorption factor, F_μ, of 1.37 was used, as discussed in Attachment DE Q6-A. This value was computed at the 95 percent probability of exceedance level based upon the results of nonlinear time-history analyses of the turbine building conducted during the probabilistic risk assessment for the Long Term Seismic Program. These analyses were performed using nonlinear analysis models of the turbine building in the east-west direction, having variable strength, stiffness, and damping properties, and subjected to a large suite of earthquake time-histories (Kennedy and others, 1988).

The results of the evaluation of the turbine building shear walls are summarized in Table DE Q6-3. The controlling section and the corresponding results are reported for each wall. The results also include the seismic margin in terms of the scale factor (FS_l) for these walls.

The controlling element of the Unit 1 turbine building was found to be wall 17 with a seismic margin of 49 percent. In Unit 2, wall 31 governs and has a seismic margin of 63 percent.

REFERENCES

Kennedy, R. P., Wesley, D. A., and Tong, W. H., 1988, Probabilistic evaluation of the Diablo Canyon turbine building seismic capacity using nonlinear time history analysis: NTS Engineering Report 1643.01, prepared for PG&E.

Table DE Q6-1

CONTAINMENT BUILDING

COMPARISON OF MAXIMUM MAGNITUDE EARTHQUAKE DEMANDS AND CONSERVATIVE DETERMINISTIC FAILURE MARGIN CAPACITIES

Wall Location	Force Component (ft/kips)	MME Demand ($x10^3$)	CDFM Capacity ($x10^3$)	Scale Factor (FS_l)
Shell	Shear	62.1	103	2.01
El 172 ft	Moment	4,240	15,700	3.88
Shell	Shear	80.1	115	1.80
El 89 ft	Moment	9,800	22,700	2.74
Crane Wall El 91 ft	Moment	1,220	2,030	1.94
Shield Wall El 91 ft	Moment	272	410	1.79
Interior Structure, Global El 91 ft	Shear	37.6	66.0	2.18

Table DE Q6-2

AUXILIARY BUILDING

COMPARISON OF MAXIMUM MAGNITUDE EARTHQUAKE DEMANDS AND CONSERVATIVE DETERMINISTIC FAILURE MARGIN CAPACITIES

North-South Walls				
Wall Location	Force Component (ft/kips)	MME Demand ($x10^3$)	CDFM Capacity ($x10^3$)	Scale Factor (FS_l)
H	Shear	10.6	13.6	1.44
El 85 ft	Moment	335	567	1.51
Auxiliary Building, Core West Walls	Shear	40.9	73.8	1.81

East-West Walls				
Wall Location	Force Component (ft/kips)	MME Demand ($x10^3$)	CDFM Capacity ($x10^3$)	Scale Factor (FS_l)
6.4 or 29.6	Shear	8.1	13.9	2.09
El 100 ft	Moment	245	414	1.69
15.7 or 20.3	Shear	25.0	32.1	1.59
El 85 ft	Moment	851	1,710	1.84
Auxiliary Building, Main Core Walls	Shear	45.0	64.2	1.76

Table DE Q6-3

TURBINE BUILDING

COMPARISON OF MAXIMUM MAGNITUDE EARTHQUAKE DEMANDS AND CONSERVATIVE DETERMINISTIC FAILURE MARGIN CAPACITIES

Wall Location	Force Component (ft/kips)	MME Demand ($x10^3$)	CDFM Capacity ($x10^3$)	Scale Factor (FS_l)
19	Shear	7.8	11.4	1.99
El 104 ft	Moment	295	380	1.73
31	Shear	11.8	15.5	1.63
El 85 ft	Moment	590	882	1.95
G	Shear	18.4	29.7	2.12
El 85 ft (U2)	Moment	703	1,040	1.96
17	Shear	9.1	11.4	1.70
El 104 ft	Moment	345	379	1.49
G	Shear	19.3	27.3	1.85
El 85 ft (U1)	Moment	738	941	1.70

ATTACHMENT DE Q6-A

CONSERVATIVE DETERMINISTIC FAILURE MARGIN APPROACH

In the additional deterministic evaluations performed for the Diablo Canyon Long Term Seismic Program, seismic capacities have been determined for representative elements of structures and components using the conservative deterministic failure margin (CDFM) approach developed under Electric Power Research Institute sponsorship (EPRI, 1988). The EPRI recommendations are summarized in Table DE Q6-A-1 below (reproduced from Table 2-5 of EPRI, 1988). Each of these recommendations is discussed below, followed by a description of its application in the additional Diablo Canyon deterministic evaluation.

Table DE Q6-A-1

SUMMARY OF CONSERVATIVE DETERMINISTIC FAILURE MARGIN APPROACH

Load Combination:	Normal + SME
Ground Response Spectrum:	Conservatively specified (84% Nonexceedance Probability)
Damping:	Conservative estimate of median damping
Structural Model:	Best estimate (Median) + Uncertainty Variation in Frequency
Soil-Structure-Interaction:	Best Estimate (Median) + Parameter Variation
Material Strength:	Code specified minimum strength or 95% exceedance actual strength if test data are available.
Static Capacity Equations:	Code ultimate strength (ACI), maximum strength (AISC), Service Level D (ASME), or functional limits. If test data are available to demonstrate excessive conservatism of code equations, then use 84% exceedance of test data for capacity equation.
Inelastic Energy Absorption:	For non-brittle failure modes and linear analysis, use 80% of computed seismic stress in capacity evaluation to account for ductility benefits, or perform nonlinear analysis and go to 95% exceedance ductility levels.
In-Structure (Floor) Spectra Generation:	Use frequency shifting rather than peak broadening to account for uncertainty, plus use median damping.

LOAD COMBINATIONS

EPRI recommendations: In the CDFM approach, the Seismic Margin Earthquake (SME) loadings are only combined with normal operating loads which would be expected to occur concurrently with the SME. Load factors of unity are used for all loadings. In other words, no conservatism is added in the load combination equations when determining margin for the SME. One exception is that for the containment (which represents the last line of defense), it is probably prudent to combine an accident pressure with normal operating loads plus the SME loads.

Diablo Canyon evaluations: For the Diablo Canyon deterministic evaluations, an accident pressure of 22 psi based on a postulated small-break loss-of-coolant-accident was used in the load combination.

STRUCTURAL RESPONSE (DEMAND)

EPRI recommendations: When computing the SME demand (structure response, or in-structure response spectra), conservatism should be introduced only at the location of greatest uncertainty, which is the specification of the ground input response spectrum, i.e., in the definition of the SME. Preferably, the SME input should be defined in terms of an 84 percent nonexceedance probability site-specific SME response spectrum.

Diablo Canyon evaluations: For the Diablo Canyon deterministic evaluations, the site-specific SME response spectrum was defined for the maximum magnitude earthquake, with a moment magnitude of 7.2 with the closest distance to the fault rupture surface of 4.5 kilometers. The horizontal response spectrum was defined at the 84 percent nonexceedance probability. The vertical response spectrum was obtained from the median ratio of vertical to horizontal spectral responses multiplied by the 84 percent nonexceedance probability horizontal response spectrum.

EPRI recommendations: With the SME conservatively defined at about the 84 percent nonexceedance probability, there is no need to add additional conservatism in the lesser uncertain response parameters in order to assure about 84 percent nonexceedance probability response values at all locations throughout the structure and for input to components. Ideally, damping, structural modeling parameters, and the soil/structure interaction evaluation should all be median-centered.

Considerable controversy exists over the damping to use in dynamic models. A conservative estimate of median damping should be selected to cover this controversy. The important point is that one should aim to use median damping and not to intentionally introduce conservatism at this point.

Diablo Canyon evaluations: For the Diablo Canyon deterministic evaluations, the following damping values were used:

Civil Structures	-	7%
Bridge Crane	-	5%
Fan Coolers Welded to Floor	-	5%
Electrical Cabinets	-	5%

EPRI recommendations: Median-centered soil/structure interaction evaluations mean that full credit should be taken for such things as vertical spatial variation of the ground motion, kinematic interaction, and scattering of energy (radiation damping) from the structure back into the ground. All of these effects should be median estimated with no intentional conservative bias. The SME should be defined at a

control point represented by either the free-ground-surface or at the top of a hypothetical stiff material outcropping.

Diablo Canyon evaluations: The Diablo Canyon soil/structure interaction analyses described in Chapter 5 of the Diablo Canyon Long Term Seismic Program Final Report (PG&E, 1988) fully comply with the above recommendations from EPRI, 1988 and were used to define the input (demand) to structure and component elements. The maximum magnitude earthquake deterministic spectrum was defined at the free-ground-surface.

EPRI recommendations: Considerable uncertainty exists in structural frequency estimates, vertical spatial variation of the ground motion, and soil/structure interaction frequency shifting effects. Each of these has substantial influence on the SME demand to components mounted on the structure (i.e., in-structure response spectra). It is unrealistic and potentially very unconservative to ignore this uncertainty and only use median-centered structural frequency modeling or median-centered soil/structure interaction analysis. The effects of structural modeling frequency shifting, soil/structure interaction frequency shifting, and vertical spatial variation of the ground motion frequency shifting on in-structure spectra should be included by appropriate parameter variations. An attempt should be made to encompass the effects of a moderate plus or minus one standard deviation parameter shifting variation on in-structure spectra. In-structure spectra generated from analyses which incorporate these parameter variations should be treated as a representative input (demand) to components. Primarily, these parameter variations result in frequency shifting of the in-structure spectra.

Diablo Canyon evaluations: Because of the stiff nature of the Diablo Canyon site and the shallow embedment of the structures, the recommendations for parameter variation from EPRI, 1988 were considered to be unnecessary. Instead, all in-structure spectra were frequency shifted $\pm$15 percent to account for frequency uncertainty. Additional spectra frequency shifting was performed to account for component frequency uncertainty. Thus, for the case of a component with moderate frequency uncertainty mounted on a structure, a total of $\pm$20 percent frequency shift was used.

STRUCTURAL CAPACITY

EPRI recommendations: Responses computed as described in the previous section have less than a 16 percent probability of being exceeded if the SME were to occur. In order to achieve a high confidence of low probability of failure (HCLPF), the structure or component seismic capacity must be conservatively estimated for comparison with the estimated demand. There should be high confidence that there is less than a 5 percent probability of failure even if this demand were reached. Since it is unlikely that the computed demand will be reached, the net effect of this approach is a HCLPF.

For failure modes evaluated by analysis, a seismic capacity estimate requires an estimate of:

- Material strength
- Static capacity or failure equation
- Inelastic energy absorption capability

Each of these parameters should be conservatively estimated to achieve the above recommended level of capacity conservatism.

Material Strength

EPRI recommendations: Material strengths used in the CDFM approach should be sufficiently conservative that there is very little likelihood that actual strengths are less than those used in the margin review. When test data are available, approximately 95 percent exceedance probability strengths should be used to achieve this goal. Otherwise, code or design specified minimum strengths should be used.

Diablo Canyon evaluations: For the Diablo Canyon deterministic evaluations, steel strengths were taken at the code specified minimum values. Thus, for Grade 40 and 60 reinforcing steel, the yield strengths used were 40 and 60 ksi, respectively. ASTM A36 steel was taken to have a yield strength of 36 ksi.

Average test strengths of either 28 or 60 days are available for the concrete mixes used at Diablo Canyon. Considering typical increases in strength with age over the first several years and material strength variability, it is considered that the median strength after several years is 1.2 times the average 28-day test strength with a logarithmic standard deviation of 0.14, or 1.1 times the average 60-day test strength with a logarithmic standard deviation of 0.12. Thus, establishing the CDFM strength $f'c_{CDFM}$ at the 95 percent exceedance probability leads to:

$$\begin{aligned} f'c_{CDFM} &= 1.2e^{-1.65(0.14)}\,\bar{f}'c_{28} = 0.95\bar{f}'c_{28} \\ f'c_{CDFM} &= 1.1e^{-1.65(0.12)}\bar{f}'c_{60} = 0.90\bar{f}'c_{60} \end{aligned} \qquad (1)$$

where $\bar{f}'c_{28}$ and $\bar{f}'c_{60}$ are the average test strengths at 28 or 60 days, respectively.

Static Capacity

EPRI recommendations: In most cases, static capacity estimates should be based on code-specified ultimate capacity approaches since there is very little possibility of failure at capacities less than given by these code equations. For concrete, the ACI ultimate strength approach with the appropriate capacity reduction factor, ϕ, included should be used. For structural steel, the AISC-Part 2 (AISC, 1980) maximum strength approach with a load factor of unity is considered appropriate. For ASME components, the Service Level D approach is adequately conservative for structural failure modes. Functional failure modes may require lesser limits. In some cases, it is known that code equations for capacity are excessively conservative. In these cases, failure capacity equations based upon actual failure test data or more rigorous evaluation may be used. However, these failure equations should not be median-centered. They should be sufficiently conservatively biased to encompass nearly all of the failure test data. Because of the scarcity of failure test data, it is often difficult to extrapolate to the 95 percent exceedance static capacity equation. Secondly, because of conservatism introduced in the material strength and inelastic energy absorption factors, it is not necessary to introduce such large conservatism in the static capacity equation for a CDFM review. Moderate conservatism (about 84 percent nonexceedance probability) is sufficient at this step.

Diablo Canyon evaluations: For the additional Diablo Canyon deterministic evaluations, the recommendations from EPRI, 1988 have been followed as illustrated by several examples discussed below.

Steel Structure Members. The AISC-Part 2 strength approach was used. When the Part 2 requirements were satisfied, the Part 2 strengths were taken as 1.7 times the Part 1 allowables. In other cases, the strength of structural members was based on the AISC-LRFD (AISC, 1986) approach with the strength

reduction, ϕ , factors defined therein.

Bolted Connections. For bolted connections, 1.7 times the AISC-Part 1 (AISC, 1980) allowables was used, even though this approach is more conservative than necessary for CDFM capacities.

Welded Connections. The strength of fillet welded connections was based on fillet weld capacity data summarized in Fisher, 1978. From this data, the median shear strength, $\breve{\tau}_w$, of the fillet weld can be defined in terms of the median ultimate strength, $\breve{\sigma}_u$, of the electrode by:

$$\breve{\tau}_w = 0.84\,\breve{\sigma}_u \tag{2}$$

with an equation logarithmic standard deviation, β_{EQN}, of 0.11. The median ultimate strength is defined in terms of the minimum code nominal tensile strength, F_{EXX}, by:

$$\breve{\sigma}_u = 1.1\,F_{EXX} \tag{3}$$

with a logarithmic standard deviation, β_σ, of 0.05. In addition, a logarithmic standard deviation, β_{FAB}, of 0.15 due to fabrication tolerances should be considered. The guidance of EPRI, 1988 that material strengths be defined at the 95 percent exceedance level and that the failure strength equation be defined at the 84 percent exceedance level was intended for ductile failure modes where additional conservatism is introduced by use of a highly conservative inelastic energy absorption factor, F_μ. For a non-ductile failure mode, such as a weld failure, 98 percent exceedance material strengths, coupled with a 95 percent exceedance static capacity equation, have been used in the Diablo Canyon deterministic evaluations for those cases where code equations have been relaxed. Thus, to achieve 98 percent exceedance material strengths coupled with a 95 percent exceedance static capacity equation, the CDFM weld capacity, $\tau_{w_{CDFM}}$, becomes:

$$\begin{aligned} \tau_{w_{CDFM}} &= (\phi_w)(f_w)(F_{EXX}) \\ \phi_w &= 1.10e^{-2.05[(.05)^2+(.15)^2]^{1/2}} = 0.80 \\ f_w &= 0.84e^{-1.65(.11)} = 0.70 \end{aligned} \tag{4}$$

or
$$\tau_{w_{CDFM}} = (0.80)\,(0.70)\,(F_{EXX}) = 0.56F_{EXX} \tag{5}$$

Equation (5) results in a fillet weld capacity equal to 1.87 times the AISC-Part 1 (AISC, 1980) allowable value.

Flexural Capacity of Concrete Shear Walls. The flexural capacity of concrete shear walls was defined by the basic ultimate flexural strength provisions of the ACI Code using a strength reduction factor, ϕ, and the reinforcing steel and concrete material strengths defined above.

$$M_u = \phi\,[A_s f_y(d - a/2) + N_u(x - a/2)] \tag{6}$$

where:

M_u = CDFM ultimate flexural capacity, in-lb
ϕ = Strength reduction factor per ACI 318-89, Section 9.3

A_s = Area of reinforcement at yield, in^2.
f_y = CDFM yield strength of reinforcement, psi
d = Distance from centroid of reinforcement at yield to extreme compression face of section, in.
a = $(f_yA_s + N_u)/0.85f_c'b$
f_c' = CDFM concrete compressive strength, psi
b = Wall thickness at compression zone, in.
N_u = Normal force on section, positive sign denotes compression, lb
x = Distance from edge of compression face to point of application of N_u, in.

Shear Capacity of Concrete Shear Walls. The CDFM shear capacity of concrete shear walls is given by Equation (G-5) of Appendix G of EPRI, 1988, which is reproduced below:

$$v_u = 6.8\sqrt{f_c'} - 2.8\sqrt{f_c'}\left(\frac{h_w}{l_w} - 0.5\right) + \frac{N_A}{4l_w t_w} + \rho_{SE} f_y \qquad (7)$$

where:

v_u = CDFM ultimate shear stress capacity, psi
f'_c = CDFM material strength of the concrete, psi
h_w = Height of the wall, in.
l_w = Length of the wall, in.
t_w = Thickness of the wall, in.
N_A = Axial load on the wall (compression positive), lb
ρ_{SE} = Effective steel reinforcement ratio as defined in Appendix G of EPRI, 1988
f_y = CDFM yield strength of the reinforcing steel, psi

Equation (7) already contains a strength reduction factor, ϕ, of 0.82 on the shear stress carried by the concrete; no additional strength reduction factor is necessary.

Shear Friction. The shear friction failure mode and its limits of applicability are discussed in Benjamin, 1983 and Corley, 1981. The strength prediction equation is stated below, and is essentially the same as the ACI Code equation (ACI, 1989, Section 11.7.4).

$$V_{SF} = \phi \mu (A_s f_y + N_u) \qquad (8)$$

where:

V_{SF} = Shear friction capacity, lb
ϕ = Strength reduction factor for shear, 0.85
μ = Coefficient of friction, equal to 1.4
A_s = Area of reinforcing steel crossing the shear crack, in^2.
f_y = CDFM yield stress of reinforcing steel, psi
N_u = Normal force perpendicular to shear crack (compression positive), lb

Tangential Shear Capacity of Concrete Containment. A considerable amount of testing has been conducted in Japan on scale models of reinforced and prestressed concrete containment structures to determine their tangential shear capacity under cyclic loadings. The results of this testing are summarized in Ogaki, 1981 and Aoyagi, 1981. Based on these references, the CDFM ultimate shear capacity, V_u,

can be obtained from:

$$V_u = \frac{\phi v_u \pi D t}{\alpha} \quad (9)$$

where:

- ϕ = Strength reduction factor of 0.85 needed to provide an 84 percent exceedance probability for this strength prediction equation
- v_u = Ultimate shear stress capacity, psi
- D = Centerline diameter of the thin cylindrical wall, in.
- t = Wall thickness, in.
- α = A factor to convert cross-sectional area to effective shear area

The effective shear area is represented by ($\pi Dt/\alpha$).

Based on inelastic finite element stress analysis, Ogaki, 1981 shows α to be a function of the ratio of the moment to the product of the shear and the cylindrical diameter (M/VD), as shown in Figure DE Q6-A-1. For (M/VD) ratios less than or equal to 0.5, $\alpha = 2.0$ is commonly used. However, as (M/VD) is increased, α is increased, reaching $\alpha = 2.5$ for (M/VD) of 1.25 or greater.

As shown in Figure DE Q6-A-2, a median estimate of v_u is given by:

$$v_u = 0.8\sqrt{f_c'} + (\rho \sigma_y)_{AVER} \leq 21.1\sqrt{f_c'} \quad (10)$$

where both v_u and f'_c are in psi units, and $(\rho\sigma_y)_{AVER}$ represents the average of the effective reinforcing steel ratios in the hoop and meridional directions. It is also shown that 84 percent of the test data lies above a line defined by $\phi = 0.85$.

The average effective steel ratio is defined by:

$$(\rho \sigma_y)_{AVER} = \frac{(\rho_h + \rho_m)}{2} f_y - \frac{(\sigma_h + \sigma_m)}{2} \quad (11)$$

where:

- ρ_h = Hoop reinforcement ratio
- ρ_m = Meridional reinforcement ratio
- f_y = Yield stress capacity of the reinforcing steel, psi
- σ_h = Containment wall hoop (tension positive) stress resulting from dead load, internal pressure, and seismic, psi
- σ_m = Meridional (tension positive) stress resulting from dead load, internal pressure, and seismic, psi

In computing σ_m, the meridional stress from the seismic overturning moment is not included because:

(1) the average meridional stress around the circumference due to this effect is zero.

(2) the overturning moment effect is already included in the test results from which Equations (9), (10), and (11) are derived.

CDFM material strengths (95 percent exceedance) defined earlier are used for f'_c and f_y in Equations (10) and (11).

Shear Capacity of Thick-Walled Cylinders. Test data on the shear strength of thick-walled cylinders is presented in Bader, 1981. Based on these data, the CDFM ultimate shear capacity is calculated as

$$V_u = \phi(v_c + v_s)A_g \tag{12}$$

where ϕ is a strength reduction factor having a value of 0.72, which adjusts the strength prediction equation to an 84 percent probability of exceedance level, v_c is the shear stress resisted by the concrete, v_s is the shear stress resisted by the hoop reinforcing steel, and A_g is the gross area of the cross-section.

Based on the data in Bader, 1981, the shear stress resisted by the concrete is dependent on the ratio of the height to the outside diameter (h/D) and is given by the following:

$$v_c = 2.2\sqrt{f_c'} \quad when\ h/D \le 0.80 \tag{13a}$$

$$v_c = [3.0 - (h/D)]\sqrt{f_c'} \quad when\ 0.80 < h/D \le 1.6 \tag{13b}$$

$$v_c = 1.4\sqrt{f_c'} \quad when\ h/D > 1.6 \tag{13c}$$

where v_c and f_c' are in units of psi. Since the tested specimens were cantilever walls, the height used in the h/D ratio above was an effective height based on the ratio of the applied overturning moment to the applied shear force.

The shear stress resisted by the reinforcing steel is assumed to be carried by the hoop bars alone and is evaluated as

$$v_s = \sum \rho_{ei} f_y \tag{14}$$

where ρ_{ei} is the effective hoop reinforcing ratio for the ith layer and f_y is the reinforcing yield stress. The effective hoop reinforcing ratio is obtained from

$$\rho_{ei} = \frac{A_{si}}{(R_{outer} - R_{inner})\,S_i} \cdot \frac{R_{si}}{R_{outer} + R_{inner}} \tag{15}$$

where A_{si} is the area of the typical hoop bar at the ith layer, S_i is the spacing of the hoop bars at the ith layer, R_{si} is the radius of the ith layer, R_{outer} is the outside radius of the cylinder, and R_{inner} is the inside radius of the cylinder.

Anchorage. The CDFM anchorage strength criteria for the Diablo Canyon deterministic evaluations were those defined in Table 6-10 of EPRI, 1988. For example, the CDFM capacity of shell-type expansion anchors was taken as the ultimate capacity defined by the manufacturer divided by 3. The CDFM capacity of cast-in-place anchors was taken as the lesser of the concrete pullout capacity defined by ACI 349-85, Appendix B, or the anchorage yield capacity defined by 1.7 times the AISC-Part 1 allowables, i.e., 34 ksi for A-307 bolts. For anchorage capacity evaluations, material strengths are as defined on page 3.

Inelastic Energy Absorption Capability

EPRI, 1988 provides the following guidance for incorporating the inelastic energy absorption capability

into a CDFM capacity evaluation:

EPRI recommendations: Nearly all structures and components exhibit at least some ductility (i.e., ability to strain beyond the elastic limit) before failure. Because of the limited energy content and oscillatory nature of earthquake ground motions, this ductility is highly beneficial in increasing the seismic margin against failure for structures and components. The inelastic energy absorption factor, F_μ, represents the ratio of the earthquake level at which a certain system ductility μ is reached to the earthquake level for which failure would be predicted by linear elastic analysis. The additional seismic margin due to this inelastic energy absorption factor F_μ should be considered in any failure margin review. Ignoring this effect will lead to unrealistically low estimates of the failure margin. It is impossible to correlate performance of structures and equipment in past earthquakes with capacities predicted by elastic analyses without considering the F_μ factor. For a CDFM review, this inelastic energy absorption should be conservatively estimated.

In most cases, it is most feasible to use linear analysis techniques. With linear analysis, the easiest way to account for the inelastic absorption capability is to multiply computed seismic stresses by a reduction factor, k, to obtain effective stresses to add to non-seismic stresses:

$$\sigma_{\text{effective seismic}} = k\sigma_{\text{seismic}} \tag{16}$$

where:

$$k = \frac{1}{F_\mu} \tag{17}$$

For all but the most brittle failure modes, k can very conservatively be chosen as being equal to 0.8 for use in Equation (16). Such a k value corresponds to $F_\mu = 1.25$, which is as low as any of the results presented in Kennedy and others, 1984 for shear wall structures. It is recommended that the reductions represented by Equations (16) and (17) be used except for brittle failure modes.

In general, the $k = 0.8$ value should be justifiable for all civil structure and component support failure modes with the possible exception of buckling. Pullout of cast-in-place anchors or failure of expansion anchor should probably be based on $k = 1.0$. If cast-in-place anchor bolt stretching governs rather than bolt pullout, $k = 0.8$ can be easily justified.

Diablo Canyon evaluations: These recommendations were adopted as follows for the Diablo Canyon deterministic evaluations.

In-plane shear and flexural failure modes of concrete shear walls and flexural failure modes of steel and concrete beams and columns are considered ductile. Buckling failures are considered non-ductile. Pullout of cast-in-place anchors, failure of expansion anchors, bond failure of reinforcing steel, and welded or bolted connection failures are considered non-ductile. Yielding of cast-in-place anchors is considered ductile. With the exception of two cases where nonlinear analyses were performed, the EPRI, 1988 recommendation of $F_\mu = 1.25$ was used for ductile failure modes and an $F_\mu = 1.0$ was used for non-ductile failure modes. Thus, unless non-ductile failure modes had CDFM capacities greater than 1.25 times those of the lowest ductile failure mode, the overall capacity was based on the lowest capacity non-ductile failure mode.

A total of 200 nonlinear, time-history analyses were performed on a model of the turbine building shear walls and the results of these analyses have been presented in Kennedy and others, 1988. Table A-1 (a reproduction of Table 2-5 from EPRI, 1988) recommends that F_μ can be based on nonlinear analysis

where the permissible ductility is limited to the 95 percent exceedance ductility level for CDFM capacity calculations. Based upon the shear wall drift limit information presented in Section 2.1.3 of Kennedy and others, 1988, the 95 percent exceedance drift capacity per story is estimated to be 0.4 percent of the story height for the worst story segment of any wall. As shown in Table 5-3 of Kennedy and others, 1988, such a drift limit corresponds to a maximum drift of 1.27 inches at the top of the 55-foot high shear walls, or 0.19 percent of the wall height. The corresponding story drift ductility, μ_s , is 9.3 and the system ductility, μ, is 6.0, as shown in Table 5.3 of Kennedy and others, 1988. For this drift, Table 5-5 of Kennedy and others, 1988 shows $F_{\mu y}$ estimates ranging between 1.58 (Spectral Averaging Method) and 1.84 (Effective Riddell-Newmark). These $F_{\mu y}$ estimates are for use with a shear wall yield capacity, V_y, and must be corrected downward by the correction factor R (Equation 5-22 of Kennedy and others, 1988):

$$R = \frac{V_u}{V_y} = 1 + S(\mu - 1) \tag{18}$$

before being used with an ultimate CDFM shear capacity, V_u as defined earlier. In Equation (18), S is the ratio of the second to first slope of a bilinear force-deflected diagram, and was set at 0.03 for all nonlinear analyses reported in Kennedy and others, 1988. With S = .03 and μ = 6.0, R becomes 1.15. Thus, a conservative CDFM estimate for F_μ becomes:

$$F_\mu = \frac{F_{\mu_y}}{R} = \frac{1.58}{1.15} = 1.37 \tag{19}$$

This F_μ = 1.37 estimate was used for the CDFM evaluation of the turbine building shear walls.

The second exception where nonlinear response was explicitly considered in lieu of use of an F_μ = 1.25 was for the case of uplift of the fuel handling bridge crane. The bridge crane must uplift a sufficient height to clear the lateral stops before it could conceivably move laterally a sufficient distance to fall. This uplift is resisted by gravity and by a hold-down beam. The uplift capacity, C , was defined by

$$C = \left[PE_{\Delta_u} + SE_H\right]^{1/2} \tag{20}$$

where PE_{Δ_u} is the potential energy associated with uplifting a CDFM uplift height, Δ_u, against the resistance of gravity, and SE_H is the strain energy capacity of the hold-down beam. Because the hold-down beam has a large unbraced span for its compression flange, this hold-down beam was considered to be potentially non-ductile, and SE_H was based on the elastic strain energy capacity absorbed prior to reaching the CDFM moment capacity, i.e., F_μ = 1.0. In this formulation, the uplift demand, D, is defined by:

$$D = [KE]^{1/2} \tag{21}$$

where KE is the uplift kinetic energy of the bridge crane based on the maximum absolute uplift velocity obtained from a linear elastic dynamic analysis of the bridge crane and its supporting structure.

CAPACITIES BASED ON SEISMIC TESTING

EPRI, 1988 provides the following guidance for determining CDFM capacities for components evaluated using seismic test results.

EPRI recommendations: Often, functional failure modes will have to be assessed using test data. Component-specific qualification or fragility test data may be used for this purpose. Alternatively, a generic equipment ruggedness spectrum (GERS) might be used. Such GERS are currently being developed by EPRI for many specific types of equipment (for example, see EPRI, 1987). The GERS are intended to represent the highest 5 percent damped test response spectrum available for a specific type of equipment for which no failures were observed. The GERS are always set lower than the lowest test response spectrum for which failures were observed, if any such failure test data exists. The GERS are sufficiently conservatively biased to cover as broad a generic equipment class as possible.

If it is assumed that either component-specific qualification test data or the applicable GERS represents an upper bound on seismic input test response spectrum for a piece of equipment, then a margin factor would clearly be needed between the computed in-structure required response spectrum and the test response spectrum (TRS) in order to achieve a HCLPF capacity. However, it should be recognized that GERS and component-specific qualification tests are often very conservatively biased estimates of the maximum seismic capability (fragility) of a piece of equipment. In most cases, the actual factor of conservatism is highly uncertain. This issue needs further investigation. The following recommendations may be too conservative. Even so, at this time, it is suggested that the following criteria be used in a seismic margin assessment review:

(1) Within the frequency range of concern, over any 20 percent frequency bandwidth (for example, 10 to 12 hertz) the average ratio of TRS to any individual frequency shifted but not broadened required response spectrum should exceed a factor of 1.3.

(2) Over frequency bandwidths corresponding to less than 20 percent frequency shift, any condition where an individual frequency shifted but not broadened required response spectrum exceeds the TRS should be individually assessed as to its consequences. It is highly unlikely that a small exceedance over a narrow frequency band could lead to functional failure.

Diablo Canyon evaluations: The Diablo Canyon deterministic evaluations made use of both GERS (EPRI, 1987, 1990a, 1990b) and component-specific qualification test data. Where either GERS or TRS are used to address functional failure modes, such as relay chatter, the CDFM capacity is given by:

$$CDFM = \frac{TRS}{1.3} \quad or \quad CDFM = \frac{GERS}{1.3} \tag{22}$$

as per the recommendations of EPRI, 1988.

However, EPRI, 1988 does not provide any guidance when seismic testing is used to assess capacities for structure failure modes. Testing experience indicates that gross structural failures of cabinets, etc., such that equipment mounted therein cannot function after the shaking has ended, is very rare and is preceded by structural anomalies (weld cracking, sheet metal tearing, screw pullout, local permanent cabinet distortion, etc.) at lower test levels. Thus, for the case of component-specific qualification tests where no structural anomalies are reported at the test level, a substantial margin beyond the test level can be expected against structural failure. In these cases, the CDFM capacity has been defined as being equal to the unfactored test response spectrum. If structural anomalies are reported during the test, then the test response spectrum is factored downward by a factor ranging between 1.2 and 1.7, depending upon the severity of the reported anomaly to define the CDFM capacity.

DETERMINISTIC SEISMIC MARGIN

Various approaches exist in the literature for defining the seismic margin. Conventionally, the seismic margin has often been defined as the ratio of the capacity, C, to the elastic computed demand, D, as follows:

$$\left[\frac{C}{D}\right] = \frac{C - \Delta C_s}{D_s + D_{NS}} \tag{23}$$

where:

- C = CDFM capacity computed in accordance with the guidance given earlier in this Attachment
- D_S = Elastic computed demand following the CDFM guidance for the deterministic seismic spectra
- D_{NS} = Concurrent non-seismic demand (loading) for all non-seismic loads in the load combination
- ΔC_S = Reduction in the capacity due to concurrent seismic loadings; for example, the shear capacity of a shear wall is reduced by the seismically induced vertical tensile load on the shear wall.

The use of $(C/D)_E$ as defined by Equation (23) to define the seismic margin has the following drawbacks:

(1) The $(C/D)_E$ represents an elastic computed capacity/demand ratio. For ductile failure modes, a $(C/D)_E$ ratio less than unity does not indicate failure, but simply indicates the element has gone inelastic.

(2) The $(C/D)_E$ ratio does not define the scale factor by which the seismic loadings can be increased and still have the element remain elastic.

To counter these drawbacks, the following definition of seismic margin (scale factor) is used:

$$FS_I = \left[\frac{C - D_{NS}}{D_s + \Delta C_s}\right] F_\mu \tag{24}$$

where F_μ is the CDFM inelastic energy absorption factor (generally 1.25 for ductile failure modes and 1.0 for non-ductile modes). The scale factor FS_I represents the amount by which the deterministic spectra can be scaled to produce a demand equal to the HCLPF capacity of a structure or component. Note that the scale factor by which seismic loadings can be increased and still have an element remain elastic is given by FS_I/F_μ. The scale factor FS_I is a more meaningful seismic margin than the C/D margin defined in Equation 23.

The CDFM seismic margin earthquake defined in terms of average 5 percent damped spectral acceleration $\bar{S}a$ over the 3 to 8.5 hertz range is:

$$CDFM\ \bar{S}a = FS_I(\bar{S}a_{3-8.5}) \tag{25}$$

where $\bar{S}a_{3-8.5}$ is the average 5 percent damped spectral acceleration for the Diablo Canyon Long Term Seismic Program deterministic spectra, or 1.94 g. Thus:

$$CDFM\ \bar{S}a = 1.94\,(FS_I) \tag{26}$$

which can be compared with the $HCLPF_{84}$ values reported in Tables 7-1 and 7-2 of PG&E, 1988 from previous fragility analyses.

REFERENCES

American Concrete Institute, 1989, Building Code Requirements for Reinforced Concrete (ACI 318-89) and Commentary-ACI 318R-89.

American Institute of Steel Construction, 1980, Specification for the Design, Fabrication and Erection of Structural Steel for Buildings: 8th Edition.

American Institute of Steel Construction, 1986, Load and Resistance Factor Design Specifications for Structural Steel Buildings: 1st Edition.

Aoyagi, Y., et al., 1981, Strength and Deformational Characteristics of Orthogonally Reinforced Concrete Containment Models Subjected to Lateral Forces: Paper J4/4, Sixth International Conference on Structural Mechanics in Reactor Technology, Paris, France.

Bader, M. and Krawinkler, H., 1981, Shear transfer in the thick walled reinforced concrete cylinders: Transactions of the 6th International Conference on Structural Mechanics in Reactor Technology, Vol J(a), paper J 4/3, Paris, France.

Benjamin, J. R. and Reed, J. W., 1983, Recommended evaluation criteria for Diablo Canyon auxiliary building walls and diaphragms, Jack R. Benjamin and Associates, Inc.

Corley, W. G., Fiorato, A. E., and Oesterle, R. G., 1981, Structural walls: ACI Special Publication SP-72.

Electric Power Research Institute, 1987, General Seismic Ruggedness of Power Plant Equipment, Palo Alto, CA.

Electric Power Research Institute, 1988, A methodology for assessment of nuclear power plant seismic margin: EPRI NP-6041.

Electric Power Research Institute, 1990a (draft), Generic Seismic Ruggedness of Power Plant Equipment: NP-5223, Revision 1.

Electric Power Research Institute, 1990b (draft), Seismic ruggedness of relays: Research Projects 1707-15 and 2925-2.

Fisher, J. W., et at., 1978, Load and resistance factor design criteria for connections: Journal of Structural Division, ASCE, Vol. 104, ST9, p. 1427-1441.

Kennedy, R. P., et al., 1984, Engineering characterization of ground motion - Task 1, effects of characteristics of free-field motion on structural response: NUREG/CR-3805, Nuclear Regulatory Commission.

Kennedy, R. P., Wesley, D. A., and Tong, W. H., 1988, Probabilistic evaluation of the Diablo Canyon turbine building seismic capacity using nonlinear time history analysis: NTS Engineering Report

1643.01, prepared for PG&E.

Ogaki, Y., et al., 1981, Shear strengths tests of prestressed concrete containment vessels: Paper J4/3, Sixth International Conference of Structural Mechanics in Reactor Technology, Paris, France.

Pacific Gas and Electric Company, 1988, Final report of the Diablo Canyon Long Term Seismic Program: Docket No. 50-275 and 50-323.

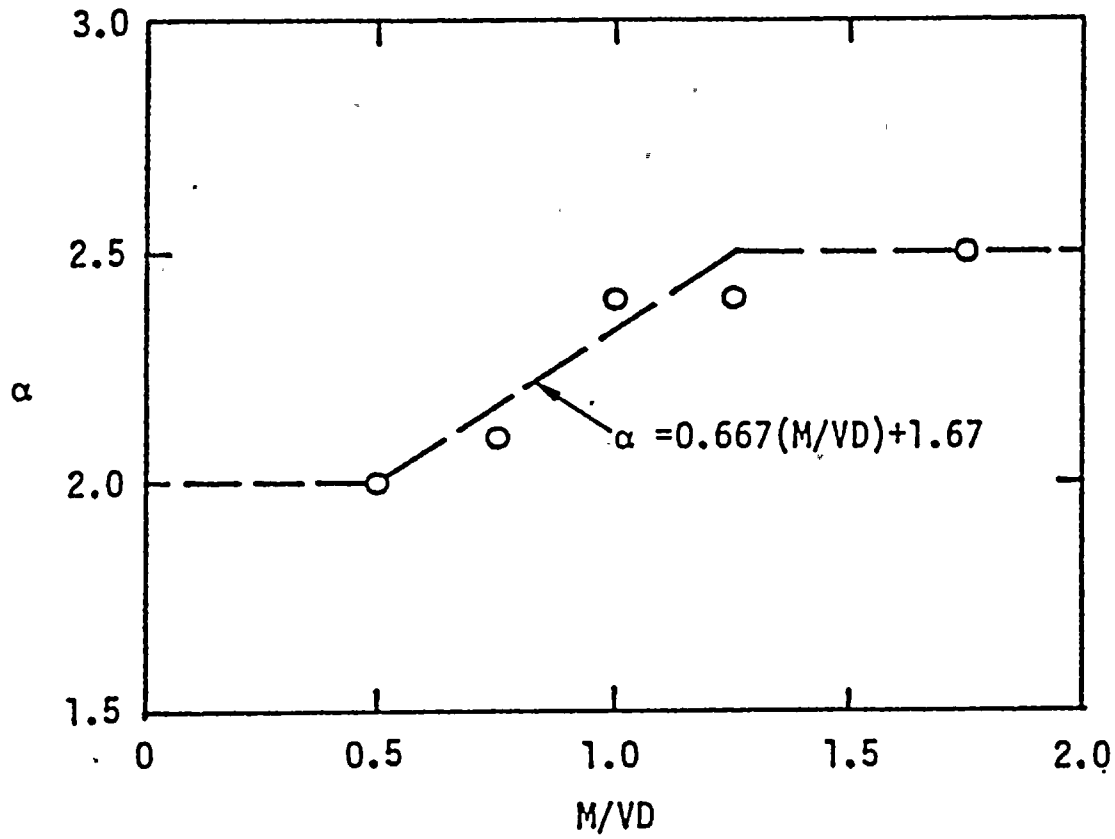

Figure DE Q6-A-1

Variation of α as a function of M/VD.

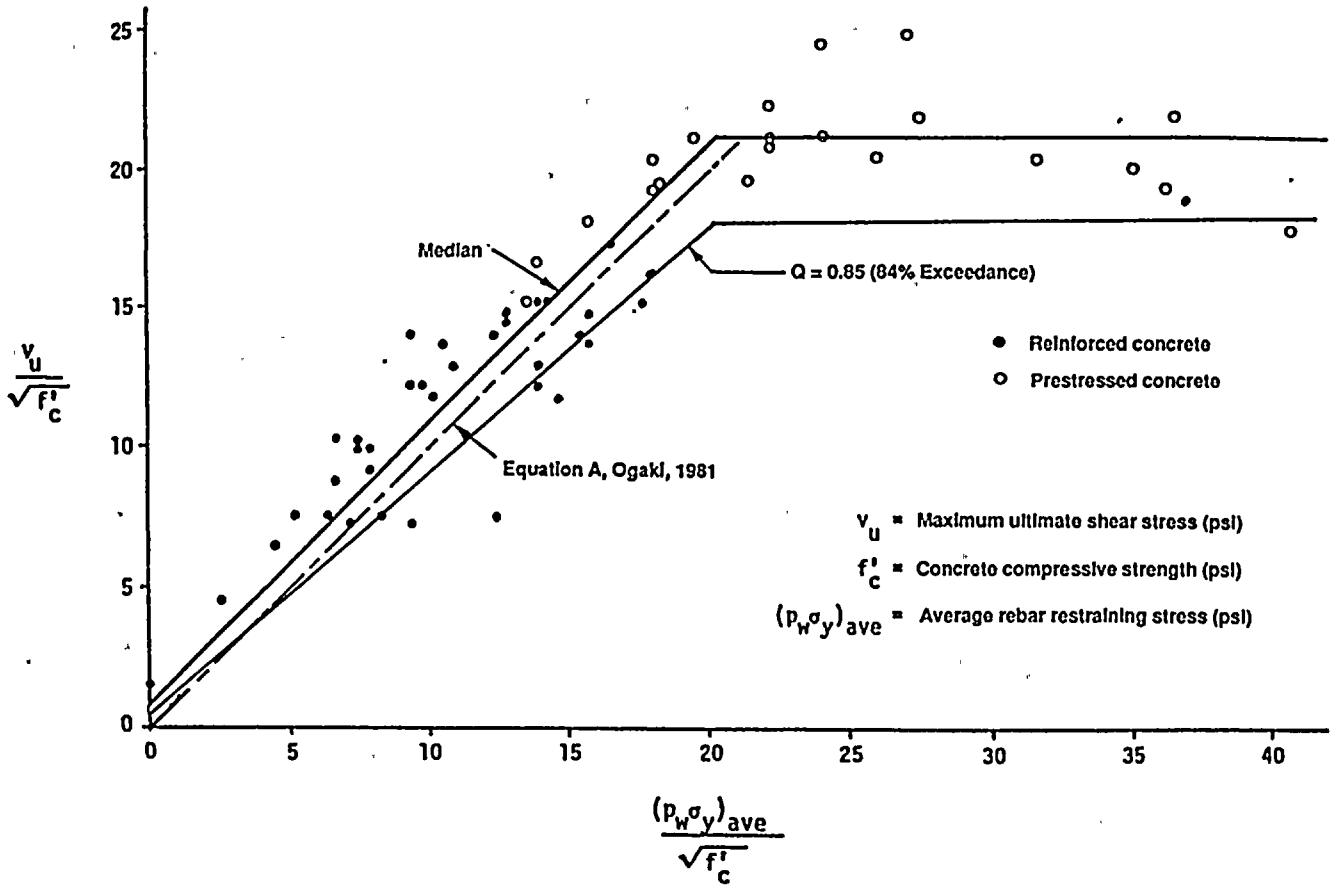

Figure DE Q6-A-2

Comparison of Japanese scale model test data to predictive formulations (from Figure 15 of Ogaki, 1981).

QUESTION DE 7

Describe the additional deterministic evaluations performed for the fuel handling building crane.

General Description of Crane

The fuel handling building crane is an electric overhead travelling crane serving both Units 1 and 2 with a rated lift capacity of 125 tons. The crane is housed in the fuel handling building steel superstructure. An elevation of the crane is shown in Figure DE Q7-1. The crane consists of two welded box-type steel bridge girders spanning between runway girders and supported on the building superstructure columns. A trolley is mounted on top of the bridge girders.

Restraints are provided to inhibit vertical movement and to prevent derailing of the bridge and the trolley from their rails. Details of the trolley and bridge girder restraints are shown in Figure DE Q7-2. Bridge derailment is prevented by horizontal beams located above the ends of the bridge. The beams are bolted to the building columns. Trolley derailment is prevented by four brackets attached to the trolley and extending under the bridge girder top flanges. Horizontal restraint bumpers are provided to transfer transverse loads from the crane bridge girders to the crane runway girders.

The maximum operating load for the crane is expected to be 80 to 100 tons, the estimated weight of the spent fuel shipping cask being lifted from the spent fuel pool. Such lifts will occur infrequently, and only when the crane trolley is positioned near the crane runway girder. When the crane trolley is positioned near the midspan of the crane bridge, cask lifting will be limited to tilt-up of the cask with its bottom supported on the floor of the cask decontamination area, resulting in a crane lift less than the cask weight. A spent fuel shipping cask will not be onsite for many years, therefore, the exact weight of the cask will not be known until spent fuel cask handling operations commence.

Crane Failure Modes

The crane system failure modes considered in selecting crane elements for evaluation for maximum magnitude earthquake local forces were as follows:

- Main hook cables (tension force)
- Crane bridge girders spanning between the crane runways (bending moment is the dominant effect)
- Crane runway girders spanning between building columns (bending moment is the dominant effect)
- Trolley vertical restraints (crane uplift)
- Crane bridge vertical restraint beams (bending moment is the dominant effect)

Bending of the crane runway girders was determined not to be a governing failure mode. Maximum magnitude earthquake forces were derived for each of the remaining crane failure modes listed above.

These selected elements are important to the load carrying capability of the crane or to its stability during a seismic event.

Seismic Loads

The maximum magnitude earthquake demand forces on the main hook cable and crane bridge girder are largest when the lifted load is equal to the rated capacity of the crane and the trolley is positioned at midspan of the bridge. In contrast, the trolley and bridge restraints were determined to be controlled by an unloaded crane with the trolley positioned at the midspan of the bridge. This condition results in the maximum uplift of the crane in the absence of the stabilizing benefit of the lifted load. The important crane modes have a much lower frequency than that of the supporting structure. Thus, the crane position does not have a significant effect on response. However, the crane was positioned between the columns of the fuel handling building superstructure for both the crane loaded and unloaded cases.

Main Hook Cable and Bridge Girder. During the Hosgri reevaluation, the main hook cable and the bridge girder responses were shown to be affected predominantly by vertical seismic loads. The horizontal seismic loads only contributed about 1 percent of the combined Hosgri loading demand. The effects of horizontal seismic loads in the direction normal to the crane runway (east-west) are small because the bridge girders are very stiff in that direction and the crane behaves very nearly as a rigid body. The effects of horizontal seismic loads in the direction parallel to the crane runway (north-south) are small because inertia loads in that direction are limited by sliding of the crane bridge wheels on the runway rails. Tests conducted during the Hosgri reevaluation demonstrated that the force required to overcome the resistance provided by the crane bridge wheel brakes is quite small. Swinging of the lifted load due to horizontal seismic motion has a negligible contribution to the demand forces on the crane because of the low frequency of the pendulum motion.

Based on the results of earlier Hosgri linear and nonlinear analyses, the maximum magnitude earthquake analysis was performed with emphasis placed on response of the crane to vertical loads. The maximum forces on the hoist cables and bridge girder were determined by response spectrum modal superposition analysis of the same dynamic linear elastic beam model used for the Hosgri reevaluation. The beam model included masses lumped along its span and a truss element to represent the hoist cables (tension and compression permitted). A lumped mass suspended at the end of the truss element was used to represent the lifted load.

The use of a linear elastic analysis model yields conservative results. During the Hosgri reevaluation, a nonlinear time-history analysis was performed of the crane with a suspended load equal to the crane rated capacity. The results of this analysis were used for the qualification of the crane. Nonlinear behavior of the hoist cables was represented by a buckling truss element (only tension forces permitted). A comparison of the nonlinear analysis results with those of a linear elastic response spectrum analysis for the Hosgri earthquake showed that the linear analysis was conservative. This was the expected result because the response of the lifted mass has a dominating effect on the crane in the linear analysis, while the nonlinear behavior of the hoist cables tends to prevent resonance of this system. Conservatism in the linear analysis results compared to the nonlinear analysis for the Hosgri reevaluation (seismic portion only) was approximately 30 to 50 percent. In the evaluation for the maximum magnitude earthquake, no credit was taken for a reduction in response as a result of the nonlinear behavior of the hoist cables.

In the linear modal superposition analysis, responses of the bridge girder and hoist cables are dominated by two modes as shown in Table DE Q7-1. These two modes are due primarily to the oscillation of the lifted mass and the bridge girder. Two percent and five percent of critical damping were used for the

"cable" mode and the "bridge" mode, respectively. The spectral accelerations at the two dominant modes were determined by scaling the Hosgri vertical spectrum at the crane runway girder by the ratio of the maximum magnitude earthquake to Hosgri vertical spectral accelerations at the ground level, at the frequencies of interest. This is considered to be valid because both the building vertical frequency and the vertical frequency of the runway girder are much greater than the significant vertical frequencies of the crane. Also, for the same reason, shifting of the peaks of the input spectra applicable at the crane runway, to account for uncertainties in the spectra, has no effect on the crane response.

Crane Trolley and Bridge Vertical Restraints. As discussed above, the crane vertical restraints are controlled by an unloaded crane. A linear elastic model was used for analysis of the unloaded crane. The linear analysis was performed to compare the results with the corresponding results of Hosgri linear analysis. The trolley was located at midspan of the bridge girder. This trolley position resulted in the maximum uplift demands on the bridge and trolley vertical restraints.

The analysis showed that the unloaded crane model can be approximated by a single-degree-of-freedom system with a frequency in the vertical direction of approximately 7.6 hertz. The fundamental mode in the vertical direction is related to bending of the bridge girder. For this reason and the reasons discussed above, the maximum magnitude earthquake demands were determined by scaling the seismic demands from the Hosgri time-history analysis by the ratio of the maximum magnitude earthquake to Hosgri spectral accelerations at the ground level, at the fundamental frequency of the girder. Four percent damping was used in the Hosgri analysis. The results were adjusted for 5 percent damping used in the current analysis. The seismic demands were then combined with the effects of gravity loads.

Comparison with Hosgri Loads and Capacities

Maximum magnitude earthquake demands, combined with gravity loads, are compared with Hosgri reevaluation demands based on linear analysis in Table DE Q7-2. The comparison shows that the demands due to maximum magnitude earthquake vertical motions and gravity loads on the bridge girders and the hoist cables are less than the corresponding Hosgri demands. For the bridge girder and the trolley vertical restraints, however, the maximum magnitude earthquake loads, combined with gravity loads, are 12 to 41 percent greater than the corresponding Hosgri loads.

A comparison of maximum magnitude earthquake demands with the member capacities derived on the basis of Hosgri reevaluation criteria is provided in Table DE Q7-3. The crane bridge demands and capacities in the table are reported in terms of interaction ratios. The demand interaction ratio was computed by using the AISC equation for axial force and bending, with 1.7 times the AISC Part 1 allowable stresses (Attachment DE Q6-A). Three components of earthquake response and gravity loads were considered. The comparison shows that maximum magnitude earthquake demands are 39 to 79 percent of the Hosgri capacities.

CDFM Capacity Evaluation

The capacities of the various elements of the fuel handling building crane were determined using the conservative deterministic failure margin approach described in Attachment DE Q6-A. For the bridge girder, an inelastic energy absorption factor of 1.25 was used. The wire rope cable capacity was taken as its minimum specified breaking strength. Since the wire rope capacity was taken as its breaking strength, an inelastic energy absorption factor was not applicable.

Comparisons of Demands to Capacities and Assessment of Seismic Margin

A comparison of maximum magnitude earthquake demands with the member capacities determined using the conservative deterministic failure margin approach is provided in Table DE Q7-4. The crane bridge demands and capacities in Table DE Q7-4 are reported in terms of interaction ratios, similar to Table DE Q7-3, except that CDFM criteria were used. For the bridge and trolley vertical restraints, the linear analysis leads to underestimation of the seismic margin because the effects of trolley and crane bridge uplift are not accounted for and failure of the restraints does not necessarily lead to failure of the crane. The nonlinear analysis described below considers these effects and is more realistic. Thus, for the bridge and trolley vertical restraints, the demand and capacity comparison, including assessment of seismic margin, are based on the results of the nonlinear analysis.

Table DE Q7-4 also lists the seismic margin in terms of the scale factor (FS_1) for the failure modes evaluated. The controlling element of the crane was found to be the bridge girder with a seismic margin of 55 percent.

Realistic Margin Considering Uplift

The crane is considered to fail when: (1) it uplifts a sufficient height to clear the lateral stop; and (2) it moves laterally a sufficient distance to fall from the crane runway. Crane bridge girder uplift is resisted by gravity and by a hold-down beam.

To determine a more realistic seismic margin against uplift of the crane (unloaded case), an energy balance technique as outlined by Hadjian, et. al., 1980, was applied. The energy demand was estimated by:

$$\text{Demand KE} = m(v_g^2 + v_i^2)/2$$

where:

- m = Mass of crane
- v_g = 84 percent probability of nonexceedance peak ground velocity of input motion
- v_i = Maximum relative velocity of the crane mass for the maximum magnitude earthquake input motion

The simplified method of calculating demand KE was validated by performing a linear elastic time-history analysis of a simplified model of the crane and computing the total energy of the system at each time step. A simplified model of the crane system consisting of two masses and two springs representing the crane and the supporting building structure was used. The model is shown in Figure DE Q7-3. The following equation was used:

$$\text{Demand KE}(t) = mv_{abs}^2/2 + R^2/(2K)$$

where:

KE(t) = Energy of the system at time t

m = Mass of crane

v_{abs} = Absolute velocity of the crane mass at time t

R = Force in the spring representing the crane at time t

K = Stiffness of the spring representing the crane

The first term in the energy equation represents the kinetic energy of the crane mass, while the second term accounts for the strain energy stored in the crane bridge. The vertical maximum magnitude earthquake input motion used was a Pacoima Dam record that was modified and scaled to match the maximum magnitude earthquake vertical ground spectrum. A comparison of the maximum energy from the time-history analysis result with that determined by Hadjian, 1980 shows close agreement.

Uplift demand, D, is defined by:

$$D = [KE]^{1/2}$$

The uplift capacity was calculated from the uplift height at failure (Δ_u). As shown in Figure DE Q7-2, the crane must uplift at least 7-1/4 inches before lateral restraint provided by the horizontal bumpers could be lost. Even at such a height, the supporting building structure must displace laterally more than 9 inches relative to the crane before the crane could fall from the runway girder. An uplift height of 4.75 inches was conservatively chosen as a HCLPF value. The energy capacity is also composed of the contribution from the bridge vertical restraint beam, but this contribution is somewhat less than the potential energy of the crane. The uplift capacity, C, was defined by:

$$C = [PE_{\Delta_u} + SE_H]^{\frac{1}{2}}$$

where PE_{Δ_u} is the potential energy associated with uplifting a CDFM uplift height, Δ_u, against the resistance of gravity, and SE_H is the strain energy capacity of the hold-down beam. Because the hold-down beam has a large unbraced span for its compression flange, the hold-down beam was considered to be potentially non-ductile, and SE_H was based on the elastic strain energy capacity absorbed prior to reaching the CDFM moment capacity, i.e., $F_\mu = 1.0$.

The uplift demands and CDFM capacities are compared in Table DE Q7-4. The scale factor computed from the energy balance technique, which also represents the seismic margin, is equal to the ratio of the uplift capacity to uplift demand. A similar energy balance calculation was performed for the trolley uplift. The scale factors for the bridge and trolley are shown in Table DE Q7-4.

Conservatisms in Seismic Evaluations

The margins reported in Table DE Q7-4 are very conservative for the reasons listed below:

- The crane was evaluated for the rated hook capacity of 125 tons concurrent with the maximum magnitude earthquake. However, the spent fuel shipping cask weight is expected to be only 80 to 100 tons.

- Cask handling operations or similar heavy lifts occur infrequently, and are highly unlikely to occur at the same time as the maximum magnitude earthquake.

- Trolley position at bridge midspan was used in the analysis although this position does not occur during handling of the loaded spent fuel shipping cask.

- Linear elastic analysis results were used for the cable and bridge girder. The linear analysis did not consider hoist cable buckling. For the Hosgri reevaluation, linear analysis resulted in seismic demands 30 to 50 percent greater than a more realistic nonlinear analysis.

If we only consider the conservatism implicit in linear elastic analysis and ignore the other conservatisms listed above, the seismic margin reported for the bridge girder in Table DE Q7-5 is likely to increase from 55 percent to over 100 percent (1.3 x 1.55 = 2.01).

REFERENCES

Hadjian, A. H. et al., 1980, Seismic analysis of structures and equipment for nuclear power plants: Design Guide No. C-2.44, Bechtel Power Corporation.

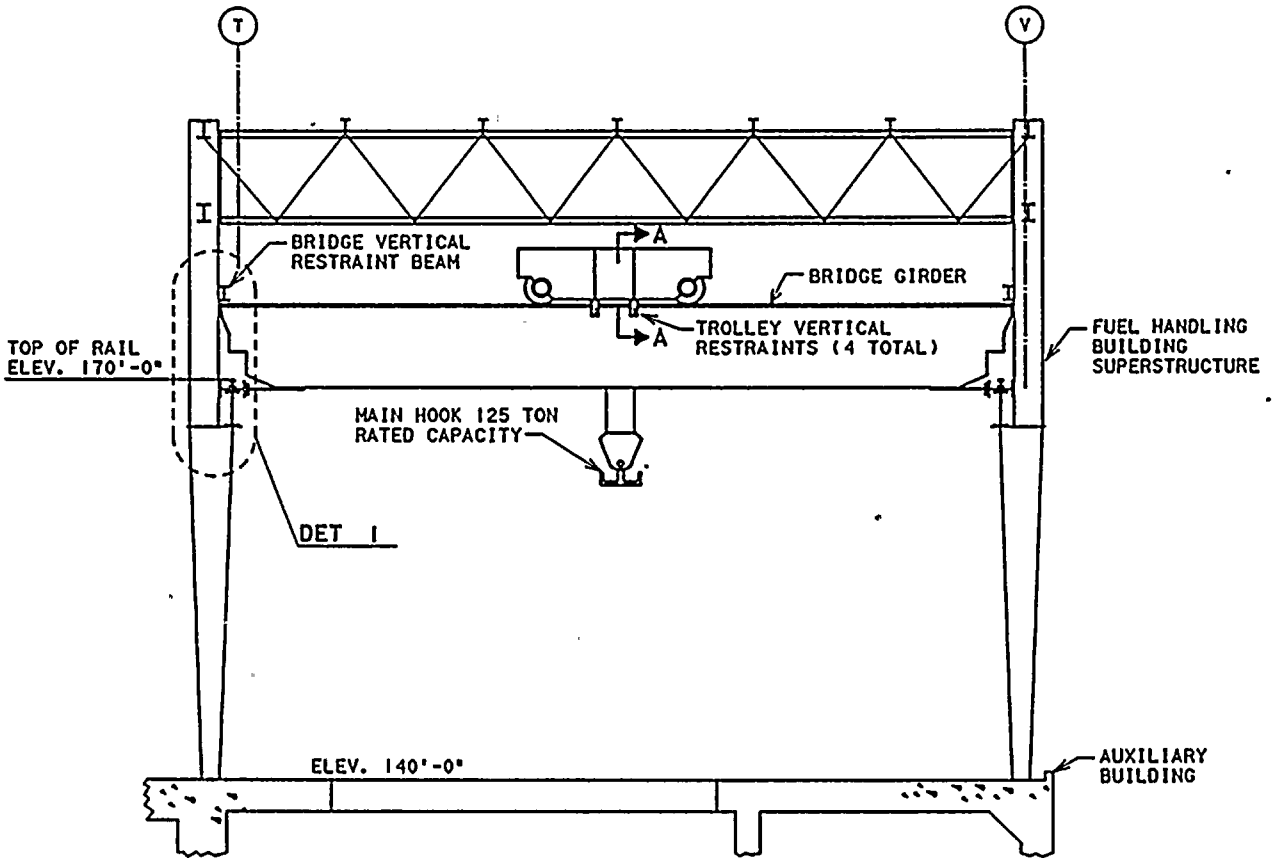

Figure DE Q7-1

Elevation view of the fuel handling building bridge crane.

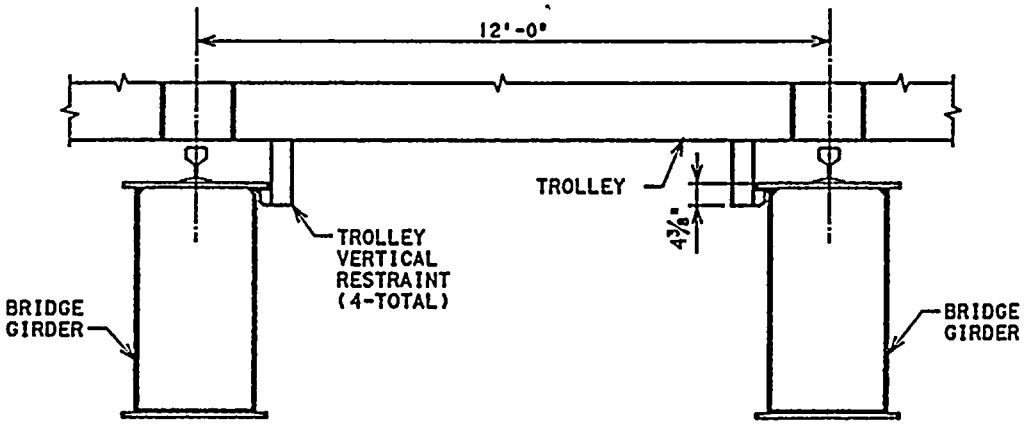

SECTION A-A

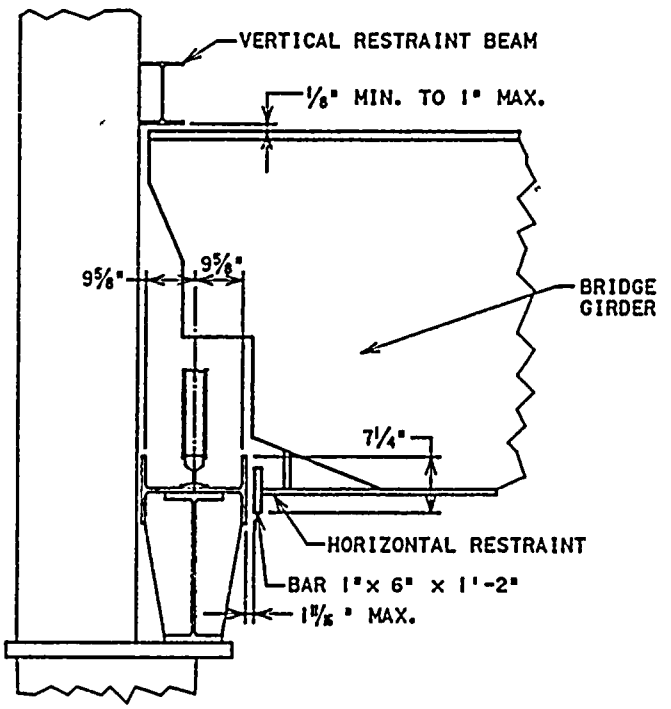

DETAIL 1

Figure DE Q7-2

Details of the fuel handling building crane trolley and bridge girder vertical restraints.

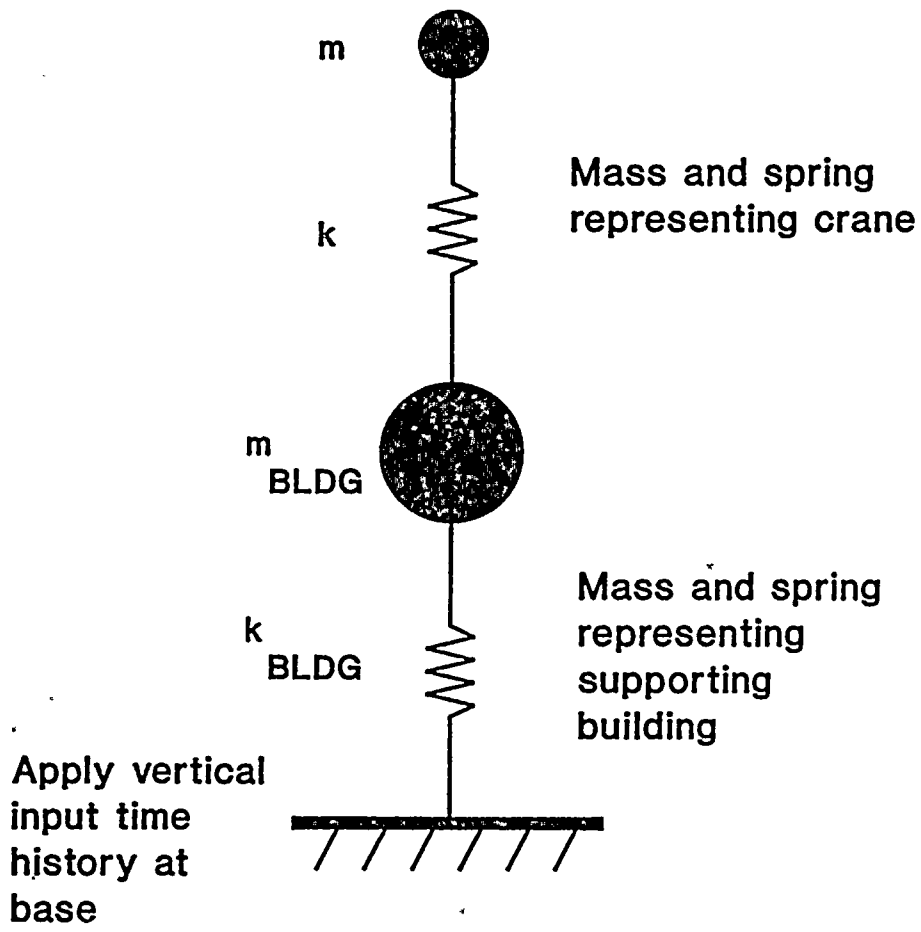

Figure DE Q7-3

Simplified dynamic model of the crane system and the supporting building structure.

Table DE Q7-1

FUEL HANDLING BUILDING CRANE

RESULTS OF LINEAR ELASTIC ANALYSIS FOR LOADED CASE

Mode	Frequency (Hz)	Effective Modal Mass (Percent)	Spectral Acceleration (g) Hosgri	MME
1	2.6	77.2	2.25	1.43
2	9.8	12.7	1.28	1.74

Table DE Q7-2

FUEL HANDLING BUILDING CRANE

COMPARISON OF MAXIMUM MAGNITUDE EARTHQUAKE AND HOSGRI EARTHQUAKE DEMANDS

Crane Element	Lifted Load (tons)	Element Force	MME Demand	Hosgri Demand
Cable	125	Tension (kips)	657	885[1]
Bridge Girder	125	Bending Moment (ft-kips)	5,190	6,460[1]
Bridge Vertical Restraint Beams	0	Reaction (kips)	14.5	10.3
Trolley Vertical Restraints	0	Reaction (kips)	12.3	11.0

NOTE:

[1] The Hosgri demand based on nonlinear analysis is 697 and 5,010 for the cable and bridge girder, respectively.

Table DE Q7-3

FUEL HANDLING BUILDING CRANE

COMPARISON OF MAXIMUM MAGNITUDE EARTHQUAKE DEMANDS AND HOSGRI EARTHQUAKE CAPACITIES

Crane Element	Lifted Load (tons)	Element Force	MME Demand	Hosgri Capacity
Cable	125	Tension (kips)	657	1,680
Bridge Girder	125	Interaction Ratio	0.794	1.00
Bridge Vertical Restraint Beams	0	Reaction (kips)	14.5	33.8
Trolley Vertical Restraints	0	Reaction (kips)	12.3	25.4

Table DE Q7-4

FUEL HANDLING BUILDING CRANE

COMPARISON OF MAXIMUM MAGNITUDE EARTHQUAKE DEMANDS AND CONSERVATIVE DETERMINISTIC FAILURE MARGIN CAPACITIES

Analysis Method	Crane Element	Lifted Load (tons)	Element Demand	MME Demand	CDFM Capacity	Scale Factor (FS_l)
Linear	Cable	125	Tension (kips)	657	1,420	2.90
	Bridge Girder	125	Interaction Ratio	0.870	1.00	1.55
Nonlinear	Bridge Resistance to Global Uplift	0	$(Energy)^{1/2}$ $(k\text{-}in)^{1/2}$	8.7	27.9	3.2
	Trolley Resistance to Uplift	0	$(Energy)^{1/2}$ $(k\text{-}in)^{1/2}$	5.1	12.4	2.4

QUESTION DE 8

Describe the procedure that was used to determine the seismic capacity of the selected equipment using the conservative deterministic failure margin approach.

Two essential equipment components required for safe shutdown of the reactor were selected for evaluation. The first was the containment fan cooler which represents the class of equipment seismically qualified for service at Diablo Canyon by structural analysis methods. The second was the diesel generator control panel which represents the class of equipment seismically qualified by dynamic test. In this evaluation, the high-confidence-of-low-probability-of-failure (HCLPF) acceleration capacity of the equipment was estimated using the conservative deterministic failure margin (CDFM) approach and presented in terms of the 5 percent damped average horizontal ground spectral acceleration averaged over the frequency range of 3 to 8.5 hertz ($\overline{Sa}_{3-8.5}$).

CONTAINMENT FAN COOLER

The containment fan cooler is located on the containment operating deck slab at elevation 140 feet. It has fundamental frequencies of approximately 23 hertz in both horizontal directions and is rigid in the vertical direction. The following failure modes were considered in the CDFM analysis:

1. Heat exchanger supply and outlet nozzles
2. Backdraft damper
3. Fan impeller (deflection)
4. Motor rotor (deflection)
5. Frame column-to-footplate weld
6. Footplate-to-embedment weld

Based upon a comparison of the factors of safety compared to code allowable or operability limits for each failure mode, the CDFM evaluation was limited to an analysis of the footplate-to-embedment weld, which by far exhibited the least safety margin. The CDFM shear capacity of this weldment (E70 electrode) was calculated to be 39,200 psi (0.56 x 70,000) using the method described in Attachment DE Q6-A (Equation 5) for welded connections.

The containment internal structure north-south and east-west floor response spectra at elevation 140 feet (Figure DE Q8-1 and Figure DE Q8-2) resulting from the 84th-percentile, site-specific ground motion due to maximum magnitude earthquake was used to determine the demand loads. The analysis accounted for the effects of soil-structure interaction but did not include the effects of ground motion incoherency. In contrast, the demand load from the vertical excitation was determined by scaling the Hosgri vertical floor spectrum at elevation 140 feet by the ratio of maximum magnitude earthquake vertical ground response to the Hosgri vertical ground response at the floor slab frequency. However, the contribution from the vertical excitation was small and the stress in the weld was dominated by the horizontal seismic input plus the piping loads.

The fundamental frequencies of the containment fan cooler were obtained from the results of a finite element model analysis of the cooler. The frequency uncertainty is, therefore, moderate and a frequency variation of $\pm$ 15 percent was used to account for this uncertainty. In addition, there is uncertainty in the actual fundamental frequency of the containment internal structure and a $\pm$ 15 percent variation was

also used to account for this uncertainty. Combining these variabilities by SRSS, a combined $\pm$ 20 percent variation about the best estimate frequency of 23 hertz ($f_{range} = 23 \pm 20\% = 18.4$ to 27.6 hertz) was used. Thus, the spectral accelerations used to establish the horizontal response were obtained from the spectra for a frequency of 18.4 hertz.

$$(Sa)_{North/South} = 1.83\,g \quad and \quad (Sa)_{East/West} = 1.70\,g$$

These accelerations, together with the contribution from piping loads (all due to seismic excitation), were used to factor the various equivalent static unit load cases to determine the stresses in the weld due to deadweight, piping loads, and the three components of earthquake motion. Combining the earthquake directional responses by the square-root-sum-of-the-squares, the shear stress in the footplate/embedment weld was calculated to be 12,230 times the average spectral horizontal ground motion acceleration averaged over the 3 to 8.5 hertz frequency range. This is expressed as:

$$\tau_{Demand} = 12{,}230\ \bar{S}a_{3\text{-}8.5}\ psi$$

The effect of ground motion incoherence in the containment internal structure was accounted for by the spectral ratio (ratio of the floor spectral acceleration including ground motion incoherency to that when ground motion incoherency is not included). At a frequency of 18.4 hertz, this ratio equals 0.96 which reduces the previously calculated demand by about 4 percent.

The HCLPF capacity of the containment fan cooler is calculated by equating the capacity shear stress to the demand shear stress:

$$(0.96)\,12{,}230\ \bar{S}a_{3\text{-}8.5} = 39{,}200\,psi$$

$$HCLPF_{CDFM} = \bar{S}a_{3\text{-}8.5} = \frac{39{,}200}{11{,}760} = 3.33\,g$$

DIESEL GENERATOR CONTROL PANEL

The diesel generator control panel is located at the basemat of the turbine building at elevation 85 feet. The panel consists of a vertical cabinet and an attached horizontal "side cabinet" (Gauge Panel) as shown in Figure DE Q8-3. The control panel is mounted on shock isolators to minimize the vibration induced by operation of the diesels. The panel is braced in the front-to-back direction by means of a framework fabricated from Unistrut members. The framework is attached to the top of the vertical cabinet and spans to the nearby structural wall.

The control panel was seismically qualified by a dynamic shake-table test. The test was conducted for the vertical cabinet only and did not include the low "side cabinet". The tested panel was mounted on plant-typical shock isolators and was supported to simulate the front-to-back bracing.

An analysis of the control panel was performed which included the effect of the attached Gauge Panel. The fundamental frequencies of the control panel both with and without the Gauge Panel are tabulated below.

Direction	Without Gauge Panel (hertz)	With Gauge Panel (hertz)
Front-to-Back	19.0	18.7
Side-to-Side	5.4	10.0
Vertical	22.0	20.1

It can be seen that the Gauge Panel has little effect on the front-to-back and vertical direction frequencies, but it causes a substantial increase in the side-to-side frequency.

Six failure modes were analyzed in the CDFM evaluation of the control panel. These were:

1. Agastat E7012 relay chatter
2. Westinghouse ARD 440 relay chatter
3. Generic Structural Failure (based on the seismic qualification test)
4. 5/8-inch control panel/isolator holdown bolts
5. 1/2-inch isolator/floor expansion anchor
6. #5 Relay mounting screws (worst configuration)

The Westinghouse ARD 440 relay chatter failure and the Generic Structural Failure were found to be the controlling failure modes.

The two important ARD 440 relays are located relatively low in the cabinet, at heights of 22 and 31 inches above the base of the interior relay subpanel. As mounted, these relays are primarily sensitive to front-to-back excitation of the panel on which they are mounted.

In order to determine the demand acceleration at the relay location, the detailed model of the combined diesel generator control panel was analyzed using the longitudinal and transverse horizontal time-histories corresponding to the 84 percent ground response spectrum. The resulting average 5 percent damped horizontal response at a node point near the center of the relay subpanel was determined (Figure DE Q8-4) for the critical front-to-back response direction. Also shown in Figure DE Q8-4 is a 5 percent damped single axis, broad-frequency fragility test response spectrum (TRS) for these relays. The ratio of TRS to the required response spectrum (RRS) is lowest at about 15.0 hertz. Over a 20 percent frequency bandwidth centered on 15.0 hertz, the average TRS is 12.5 g and the average RRS is 5.6 g. Accounting for the effect of the ground motion incoherence factor of 0.8 (Figure DE Q8-5) in the front-to-back cabinet response, the demand horizontal spectral acceleration is:

$$CDFM\ Demand_{13.5-16.5} = 0.8\,(5.6g) = 4.48\,g$$

and the corresponding CDFM capacity is:

$$CDFM\ Capacity_{13.5-16.5} = \frac{TRS_{13.5-16.5}}{1.3}\ (Attachment\ DE\ Q6\text{-}A)$$
$$= \frac{12.5\,g}{1.3} = 9.62\,g$$

Thus, the seismic margin scale factor (FS_I) becomes:

$$FS_I = \frac{CDFM\ Capacity}{CDFM\ Demand} = \frac{9.62\,g}{4.48\,g} = 2.15$$

and the CDFM HCLPF seismic margin earthquake level is:

$$HCLPF_{CDFM} = FS_I \cdot \bar{S}a_{3-8.5} = 2.15\,(1.94\,g) = 4.17\,g$$

where $\bar{S}a_{3-8.5}$ is the 84 percent average ground horizontal spectral acceleration from 3 to 8.5 hertz which is equal to 1.94 g.

The vertical panel is supported in the front-to-back direction, and thus the control panel essentially responds structurally to side-to-side and vertical excitations. Further, the test response in the side-to-side direction represents the least overtest compared to the seismic demand. Thus, the structural capacity of the cabinet was based on the side-to-side overtest.

The qualification test included only the vertical cabinet with a side-to-side frequency of 5.4 hertz. Thus, the structural elements of the control panel experienced accelerations consistent with the Test Response Spectrum (Figure DE Q8-6) at approximately 5.4 hertz. However, the addition of the Gauge Panel increases the side-to-side frequency to approximately 10 hertz. Therefore, the demand accelerations must be evaluated at the fundamental frequency of the combined cabinet. Since the 5.4 hertz frequency of the tested configuration was determined by test, the uncertainty in the actual vertical cabinet-only frequency is reduced and is characterized by a $\pm$10 percent variation. In contrast, the combined cabinet fundamental frequency was determined by finite element model analysis for which a $\pm$ 15 percent variation should be used.

$$5.4 \text{ hertz} \pm 10\ \% = 4.9 \text{ to } 5.9 \text{ hertz}$$

$$10 \text{ hertz} \pm 15\ \% = 8.5 \text{ to } 11.5 \text{ hertz}$$

The acceleration capacity of the diesel generator control panel was evaluated from the test response spectra over the 4.9 to 5.9 hertz range and equated to the demand acceleration evaluated at 8.5 hertz.

From the Test Response Spectrum, Sa_{TRS} (3%) = 2.82 g average over 4.9 to 5.9 hertz.

Thus, the capacity acceleration for the control panel is $Sa_{Capacity}$ = 2.82 g .

From the 84 percent horizontal ground response spectrum, $\bar{S}a_{3-8.5}$ = 1.94 g.

Also, at 8.5 hertz

$$Sa_{5\%} = 1.80\,g$$

$$Sa_{3\%} = 1.80\ (2.46/2.12) = 2.09\,g$$

The numbers in parenthesis convert $Sa_{5\%}$ to $Sa_{3\%}$ at 8.5 hertz (Newmark, 1978).

The demand acceleration is then

$$Sa_{3\%} = 2.09 \left(\bar{S}a_{3\text{-}8.5}/1.94\right) = 1.08\ \bar{S}a_{3\text{-}8.5}$$

Equating the demand and capacity accelerations:

$$1.08\ \bar{S}a_{3\text{-}8.5} = 2.82\ g$$

$$HCLPF_{CDFM} = \bar{S}a_{3\text{-}8.5} = \frac{2.82}{1.08} = 2.62\ g$$

REFERENCES

Newmark, N. M. and Hall, W. J., 1978, Development of criteria for seismic review of selected nuclear power plants: NUREG CR-0098.

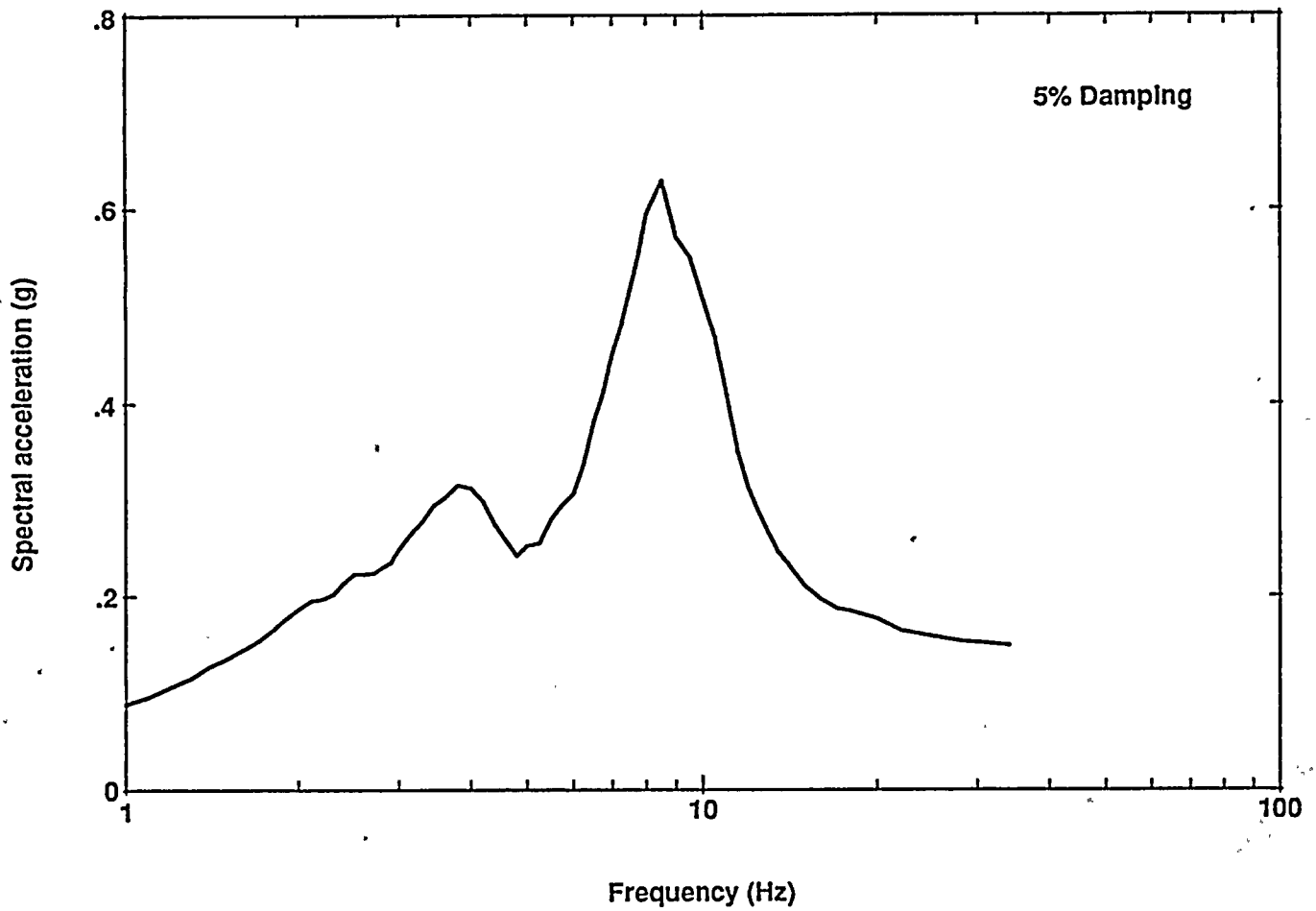

Figure DE Q8-1

Floor response spectrum at elevation 140 feet for the north-south response of the containment internal structure for the maximum magnitude earthquake ground motion.

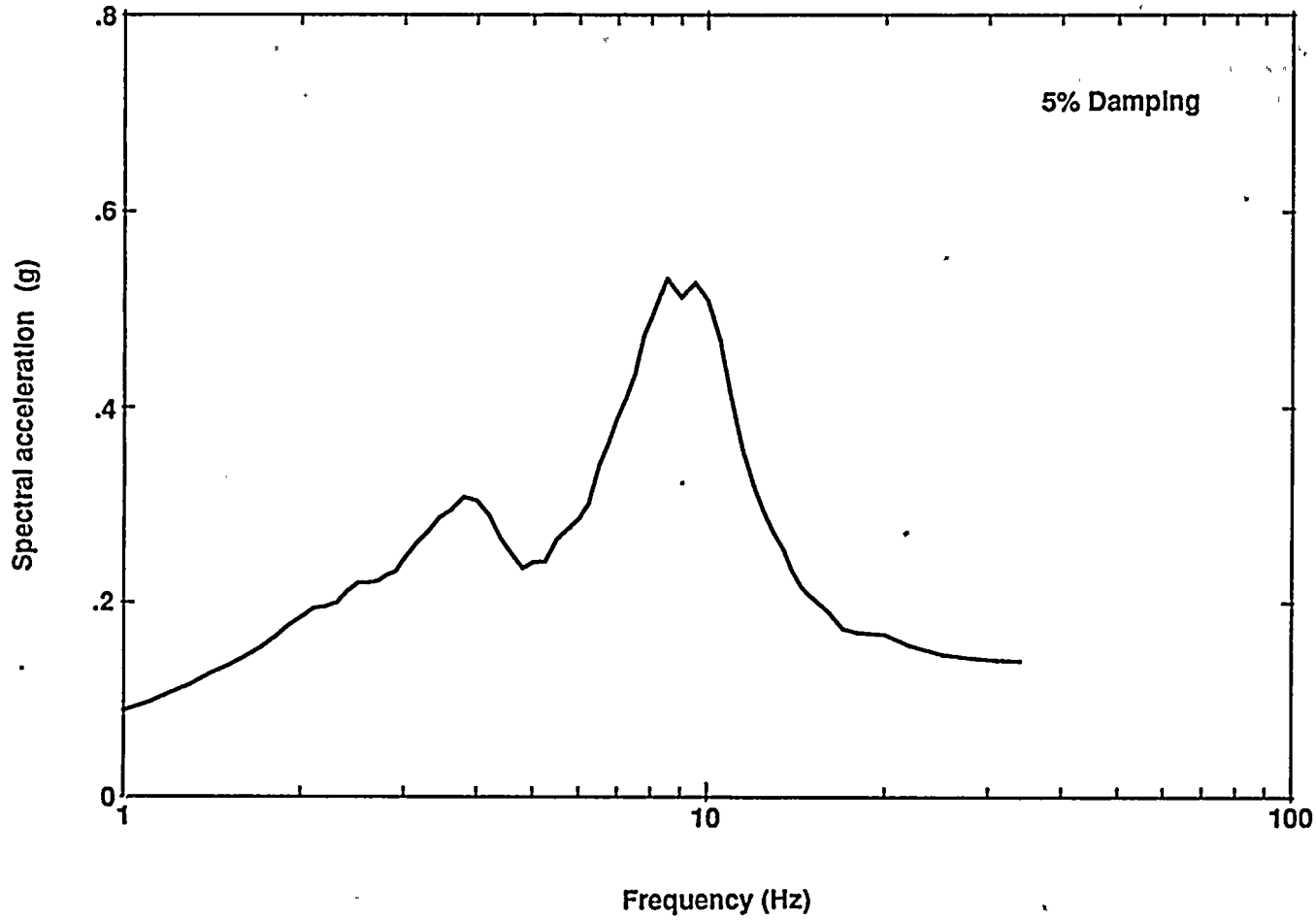

Figure DE Q8-2

Floor response spectrum at elevation 140 feet for the east-west response of the containment internal structure for the maximum magnitude earthquake ground motion.

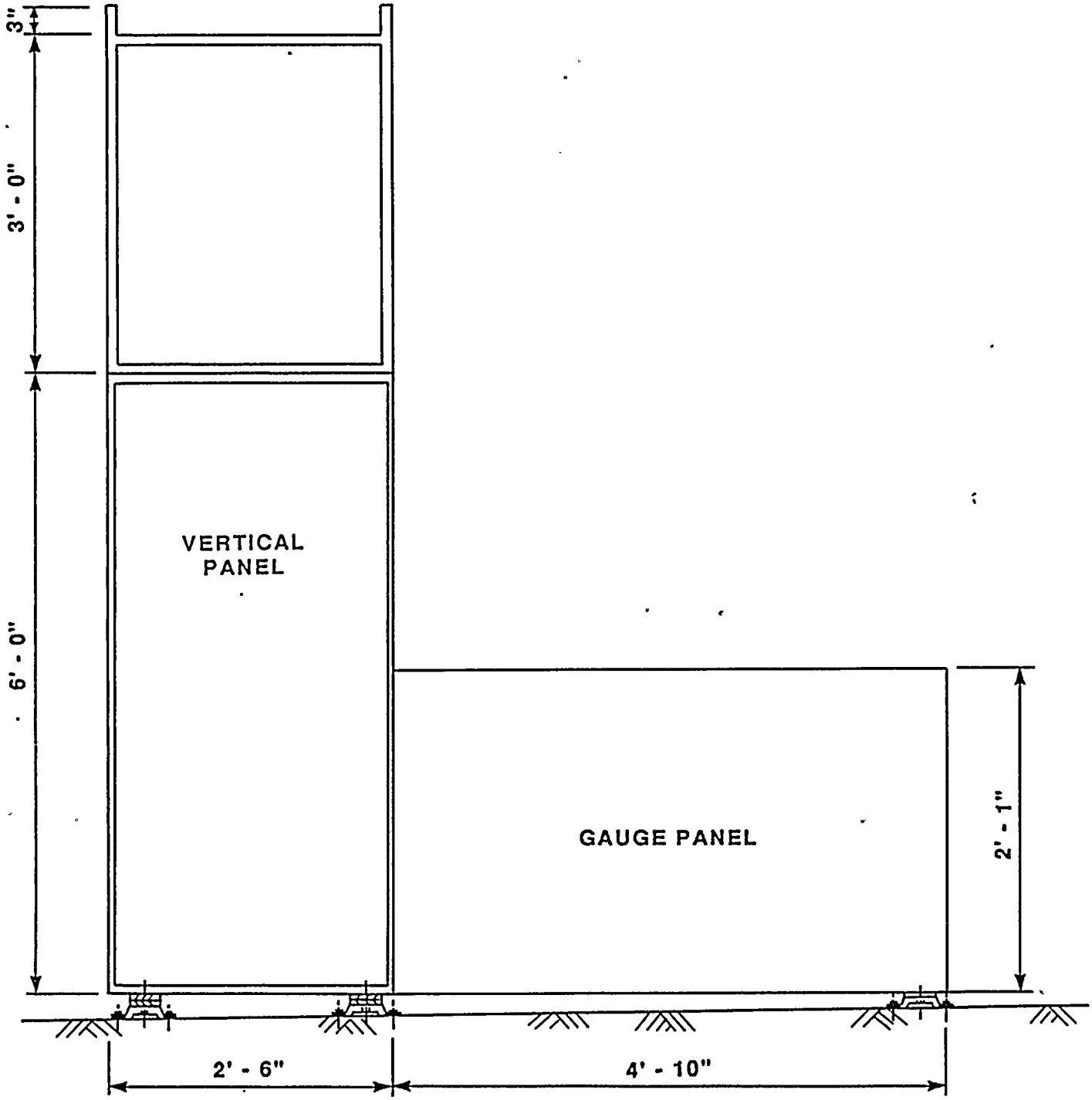

Figure DE Q8-3

Elevation of the diesel generator control panel.

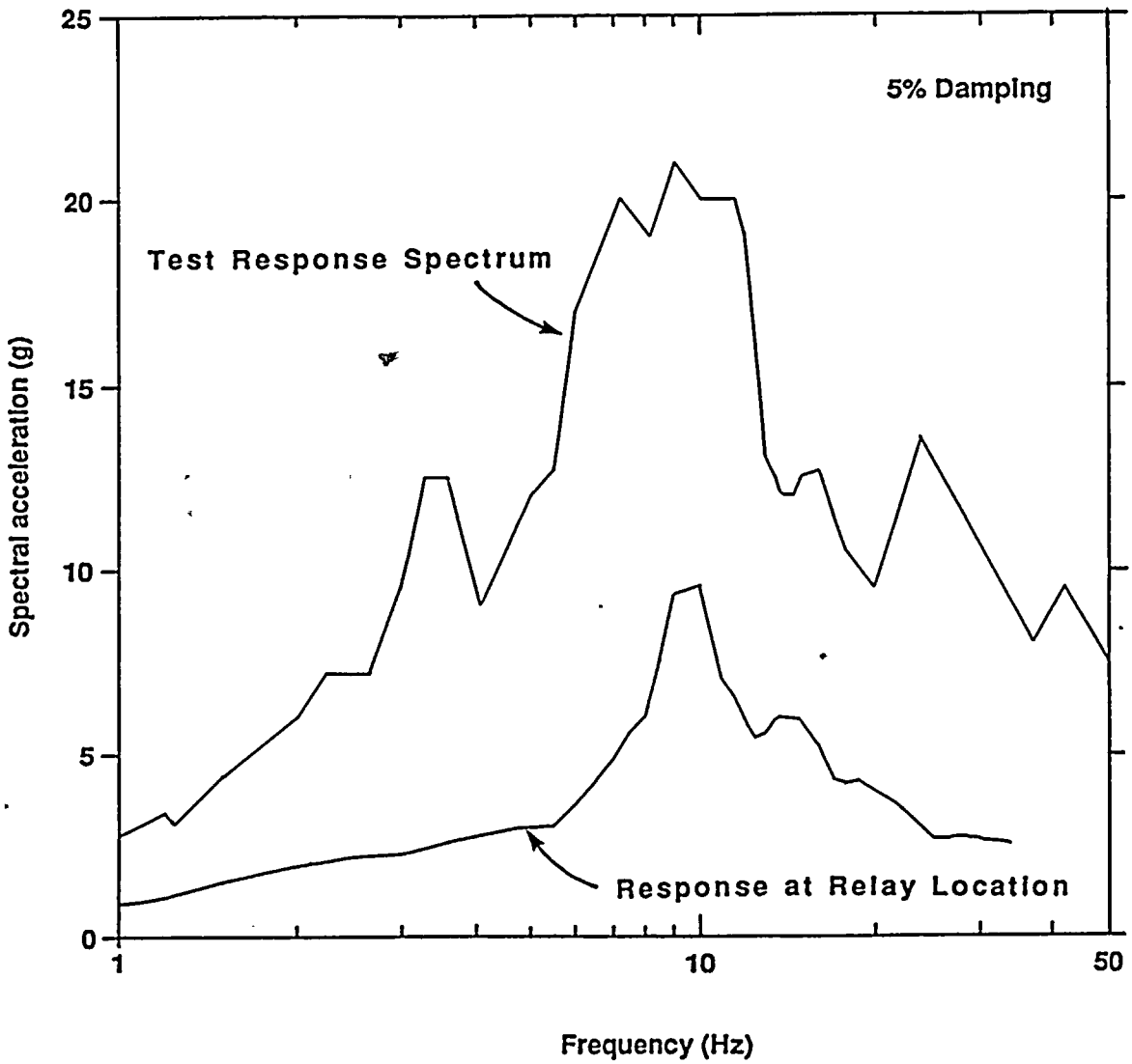

Figure DE Q8-4

Front-to-back response at relay location for maximum magnitude earthquake horizontal ground motion and test response spectrum (TRS) of Westinghouse ARD 440 relay.

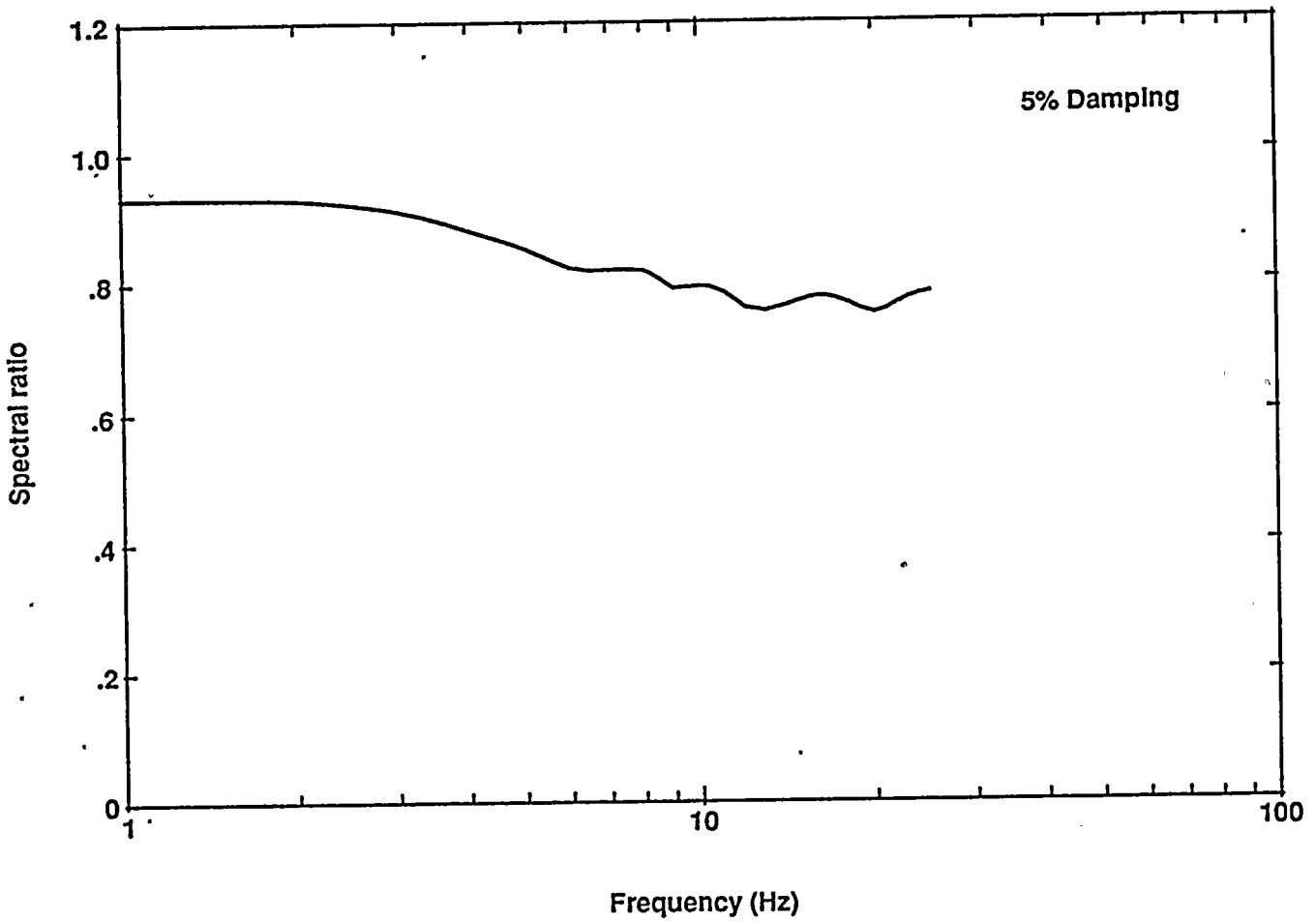

Figure DE Q8-5

Ground motion incoherency factor at elevation 85 feet, diesel generator location, north-south direction.

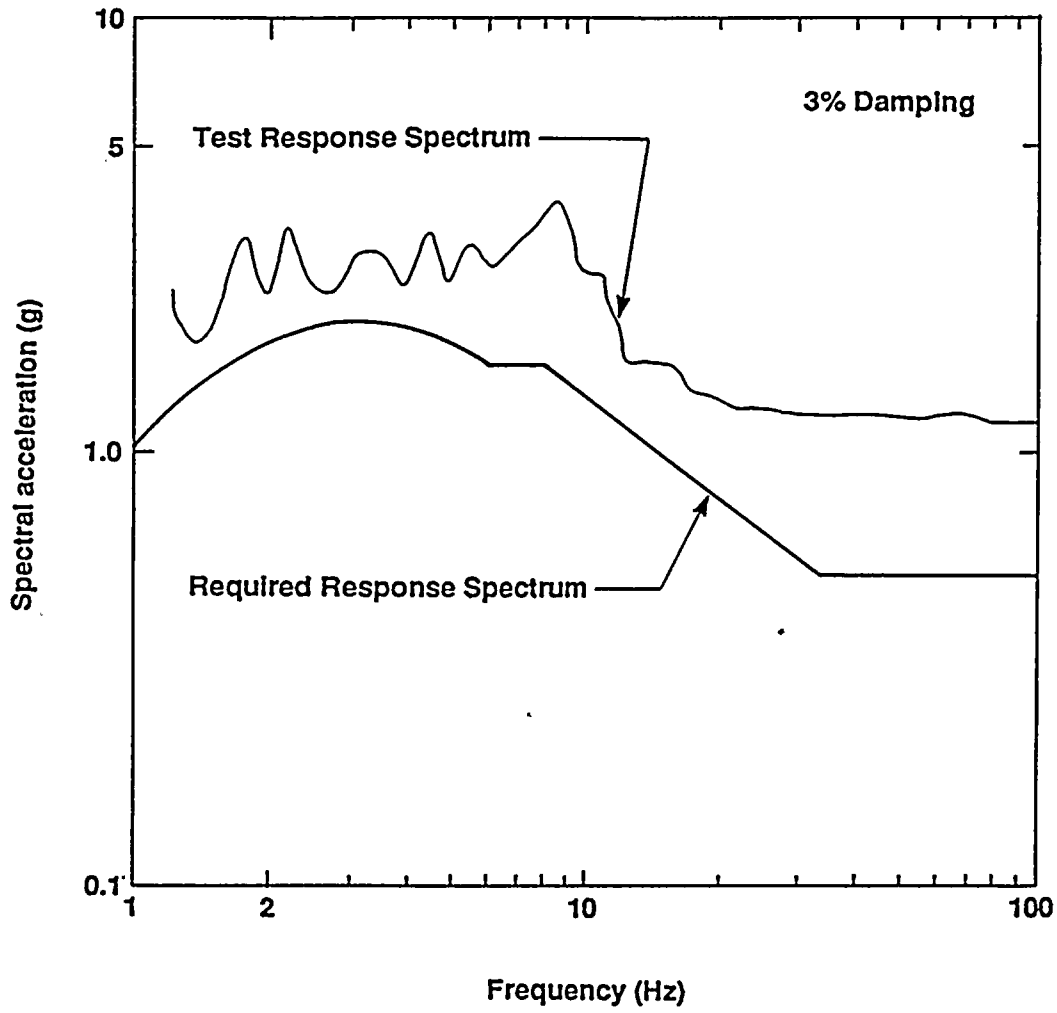

Figure DE Q8-6

Required response spectrum (RRS) and test response spectrum (TRS) for Hosgri qualification of the diesel generator control panel.

QUESTION DE 9

Develop conclusions based on the work performed for the additional deterministic evaluations of selected Plant structures and equipment.

Two approaches for computing high-confidence-of-low-probability-of-failure (HCLPF) seismic capabilities of structures and components have been recommended (Prassinos, 1986). One of these approaches is called the fragility analysis method and entails estimating the HCLPF capacity from an estimate of the median and variability of the seismic capability of the component. The other approach is called the conservative deterministic failure margin (CDFM) approach and entails performing a single deterministic seismic capability evaluation using conservative parameter estimates selected in accordance with the guidance originally specified in Kennedy, 1985. Since we had already performed fragility analyses for all structures and components identified as being important to seismic risk in the Diablo Canyon seismic probabilistic risk assessment, we elected to use the fragility analysis method to define $HCLPF_{84}$ seismic capacities of these structures and components for comparison with the 84 percent nonexceedance probability site-specific ground motion (PG&E, 1988, Chapter 7).

In this volume, CDFM seismic capacities have been calculated for selected Plant structures and a sample of components, including both the structure (turbine building) and component (diesel generator control panel) that were identified as having the lowest HCLPF capability of all components important to seismic risk in PG&E, 1988. Since the diesel generator control panel was an example of a component qualified by test, the containment fan cooler was evaluated as an example of a component qualified by analysis. Although a fragility estimate was not developed for the fuel handling building crane during the Diablo Canyon probabilistic risk assessment, this component was included because it is an example of a component whose seismic capability is almost totally governed by the vertical component of the site-specific ground motion.

The CDFM seismic capacities for the selected structures and components are presented in Table DE Q9-1. This table also includes the $HCLPF_{84}$ capacities of these structures and components that were reported in PG&E, 1988. In this table, both the $HCLPF_{84}$ and CDFM capacities are reported in terms of the 5 percent damped average spectral acceleration (Sa) between 3 and 8.5 hertz for the free-field horizontal ground motion. To define the seismic margin, these values are to be compared with the maximum magnitude earthquake Sa of 1.94 g.

In Chapter 7 of PG&E, 1988, it was stated that based upon the deterministic studies summarized therein, the 14 percent seismic margin computed for the turbine building based upon a $HCLPF_{84}$ capacity of 2.21 g was too low and was most likely in excess of 40 percent. The CDFM computed seismic capability reported herein shows that the seismic margin for the turbine building is approximately 49 percent, or substantially better than the 14 percent margin reported in PG&E, 1988.

It is concluded from the studies in PG&E, 1988 and these additional deterministic evaluations that, when based upon identical information, the $HCLPF_{84}$ capacities compare reasonably well with the CDFM capacities.

The net result of an increase in the turbine building $HCLPF_{84}$ capacity from 2.21 g to 2.89 g would be a slight (probably negligible) reduction in the seismic risk reported in PG&E, 1988. From a fragility standpoint, the seismic risk reported in PG&E, 1988 remains valid.

The CDFM seismic capabilities reported herein confirm that the turbine building and the diesel generator control panel remain the structure and component, respectively, with the least seismic margin of all elements identified in the Diablo Canyon probabilistic risk assessment as being important to seismic risk. The CDFM seismic capabilities confirm that the high-confidence-of-low-probability-of-failure seismic margin for Diablo Canyon is at least 40 percent greater than the 84 percent nonexceedance probability maximum magnitude earthquake ground motion defined for the site.

When considering the seismic margins developed in these deterministic evaluations, it should be noted that the 84 percent probability of nonexceedance site-specific spectrum used in these comparisons is very conservative. The ratio of the 84 to 50 percent spectrum is approximately 1.5. Also, there is margin above the conservative $HCLPF_{84}$ capacity values. The median capacity, which corresponds to the 50 percent probability of exceedance, is generally at least a factor of 2 greater than the $HCLPF_{84}$ capacity. For example, even when the $HCLPF_{84}$ spectral acceleration equals the average spectral acceleration for the 84 percent, site-specific spectrum (that is, there is a 0 percent margin), the median capacity will still be approximately a factor of 3 (2 x 1.5) above the 50 percent site-specific spectrum. Thus, a 0 percent deterministic margin obtained in this manner corresponds to a very remote possibility of failure.

PG&E concludes that the Diablo Canyon Power Plant has adequate seismic margin to withstand the maximum magnitude earthquake ground motions.

REFERENCES

Electric Power Research Institute, 1988, A methodology for assessment of nuclear power plant seismic margin: EPRI NP-6041.

Kennedy, R. P., 1985, Various types of reported seismic margins and their use, Proceedings: EPRI/NRC workshop on nuclear power plant reevaluation to quantify seismic margins, EPRI NP-4101-SR, Electric Power Research Institute.

Pacific Gas and Electric Company, 1988, Final report of the Diablo Canyon Long Term Seismic Program: U. S. Nuclear Regulatory Commission Docket No. 50-275 and 50-323.

Prassinos, P. G., Ravindra, M. K., and Savy, J. B., 1986, Recommendations to the Nuclear Regulatory Commission on trial guidelines for seismic margins reviews of nuclear power plants: NUREG/CR-4482, Lawrence Livermore National Laboratory.

Table DE Q9-1

STRUCTURE AND EQUIPMENT HCLPF CAPACITIES

	HCLPF Spectral Acceleration Capacity (g)[1]	
Structure/Equipment	Chapter 7 LTSP Final Report	1990 CDFM Evaluations
	$HCLPF_{84}$[2]	CDFM[2]
Containment Building	4.01	3.49
Containment Internal Structure	3.58	3.47
Auxiliary Building	3.19	3.41
Turbine Building	2.21	2.89
Fuel Handling Building Crane	N/A	3.0
Containment Fan Cooler	3.38	3.33
Diesel Generator Control Panel		
Relay Chatter	4.90	4.17
Structural	2.69	2.62

NOTES:

1 Values are referenced to average spectral acceleration between 3 to 8.5 hertz for free-field motions.

2 The values are to be compared with the site-specific ground motion demand $\bar{S}a_{3-8.5\ hertz} = 1.94\ g$.